

# The Eocene carbonate platforms of the Ghomaride Domain (Internal Rif Zone, N Morocco): a segment of the westernmost Tethys

Manuel Martín-Martín<sup>a,\*</sup>, Josep Tosquella<sup>b</sup>, Francesco Guerrera<sup>c</sup>, Alí Maaté<sup>d</sup>, Rachid Hlila<sup>d</sup>, Soufian Maaté<sup>e</sup>, Mario Tramontana<sup>c</sup>, Eline Le Breton<sup>f</sup>

<sup>a</sup> Departamento de Ciencias de la Tierra y Medio Ambiente, University of Alicante, Alicante, Spain

<sup>b</sup> Departamento de Ciencias de la Tierra, University of Huelva, Huelva, Spain

<sup>c</sup> Ex-Dipartimento di Scienze della Terra, della Vita e dell'Ambiente (DiSTeVA), Università degli Studi di Urbino Carlo Bo, Urbino, Italy

<sup>d</sup> Laboratoire de Géologie de l'Environnement et Ressources Naturelles, FS, Abdelmalek Essaâdi University, B.P. 2121, Mhannech II, 93002 Tetouan, Morocco

<sup>e</sup> Université Moulay Ismaïl, Laboratoire de Géologie Appliquée, Faculté des Sciences et Techniques, BP. 509, Boutalamine, 52000 Errachidia, Morocco

<sup>f</sup> Department of Earth Sciences, Institute for Geological Sciences, Freie Universität Berlin, Berlin, Germany

## ARTICLE INFO

### Article history:

Received 30 March 2023

Received in revised form 9 May 2023

Accepted 10 May 2023

Available online 18 May 2023

Editor: Dr. Brian Jones

### Keywords:

Carbonate platforms

Larger benthic foraminifera

Ypresian-Bartonian

Palaeoenvironmental evolution

Westernmost Tethys

## ABSTRACT

The Eocene platform deposits in the Moroccan Ghomarides have been studied. These marine carbonate platforms were located in the westernmost Tethys approximately 30°N and 0°–10°W during the Cuisian to Bartonian. The study includes observations from fossiliferous assemblages (such as larger benthic foraminifera and colonial corals), their palaeoenvironment as well as rock texture and fabric. Eight microfacies were identified that represent different ramp environments in a 'distally-steepened carbonate ramp' type of platform. The studied deposits are organised into a transgressive succession composed of three sedimentary cycles: lower Cuisian, middle Cuisian and middle Lutetian to Bartonian. In the lower cycle, photic inner to mid ramp environments in mesotrophic conditions were prevalent. In the second cycle, photic inner ramp (sea-grass) to mid ramp environments in mesotrophic to oligotrophic conditions were observed. The upper cycle, which is more extensive and variable, represents mesophotic mid ramp to aphotic slope environments and changes gradually from oligotrophic to eutrophic conditions. During the Eocene, larger benthic foraminifera were dominant overtaking the zooxanthellate corals in the Tethys regions. Nevertheless, our study and the performed comparison with other Tethyan sectors have revealed that in some areas both coexisted in similar proportions. In some western Tethys regions close to the Atlantic Ocean, coinciding with areas influenced by upwelling currents, larger benthic foraminifera and coral build-ups were replaced by oyster reefs. The Ghomaride Domain represents an intermediate case between fossil assemblages of the northern Tethyan margin and eastern sector of the southern margin of the Tethys, with a dominance of larger benthic foraminifera but with a certain presence of corals as well. A good correlation exists between Eocene warm intervals and carbonate platform deposits in these domains. Contrarily, during cooling ones shallowing and gaps in the sedimentation are registered. Two anomalies have been detected in the Ghomaride Domain during Ypresian and Bartonian times indicating particular climatic conditions or local tectonic interferences.

© 2023 The Author(s). Published by Elsevier B.V. This is an open access article under the CC BY-NC-ND license (<http://creativecommons.org/licenses/by-nc-nd/4.0/>).

## 1. Introduction

The Eocene was a warm climate period with a set of short-lived hyperthermal events widely studied due to their important repercussions on the planet (Kennett and Stott, 1991; Dickens et al., 1977; Zachos et al., 2001; Bohaty et al., 2009; Rivero-Cuesta et al., 2020). The most recognised events for their consequences on life (Fig. 1) were the Palaeocene–Eocene thermal maximum at around 55.5 Ma (Kennett and Stott, 1991; Koch et al., 1992; Thomas and Shackleton,

1996), the early Eocene climatic optimum at 53–50 Ma (Zachos et al., 2001, 2008), and the middle Eocene climatic optimum at 41–40 Ma (Bohaty and Zachos, 2003; Zachos et al., 2008).

These hyperthermal events brought about a significant increase in average global Eocene temperatures, leading to major atmospheric, oceanographic, and environmental disturbances, as noted by Kennett and Stott (1991), Koch et al. (1992), Zachos et al. (1993), Thomas and Shackleton (1996), Zachos et al. (2001) and Pujalte et al. (2003). Some of the main consequences along this warm climate period were: (i) a rise in the greenhouse effect, resulting in an increase in average temperatures; (ii) changes in marine water chemistry and ocean currents; (iii) apparition of exotic planktic foraminiferal forms, (iv) extinctions of deep-sea benthic

\* Corresponding author.

E-mail address: [manuel.martin@ua.es](mailto:manuel.martin@ua.es) (M. Martín-Martín).

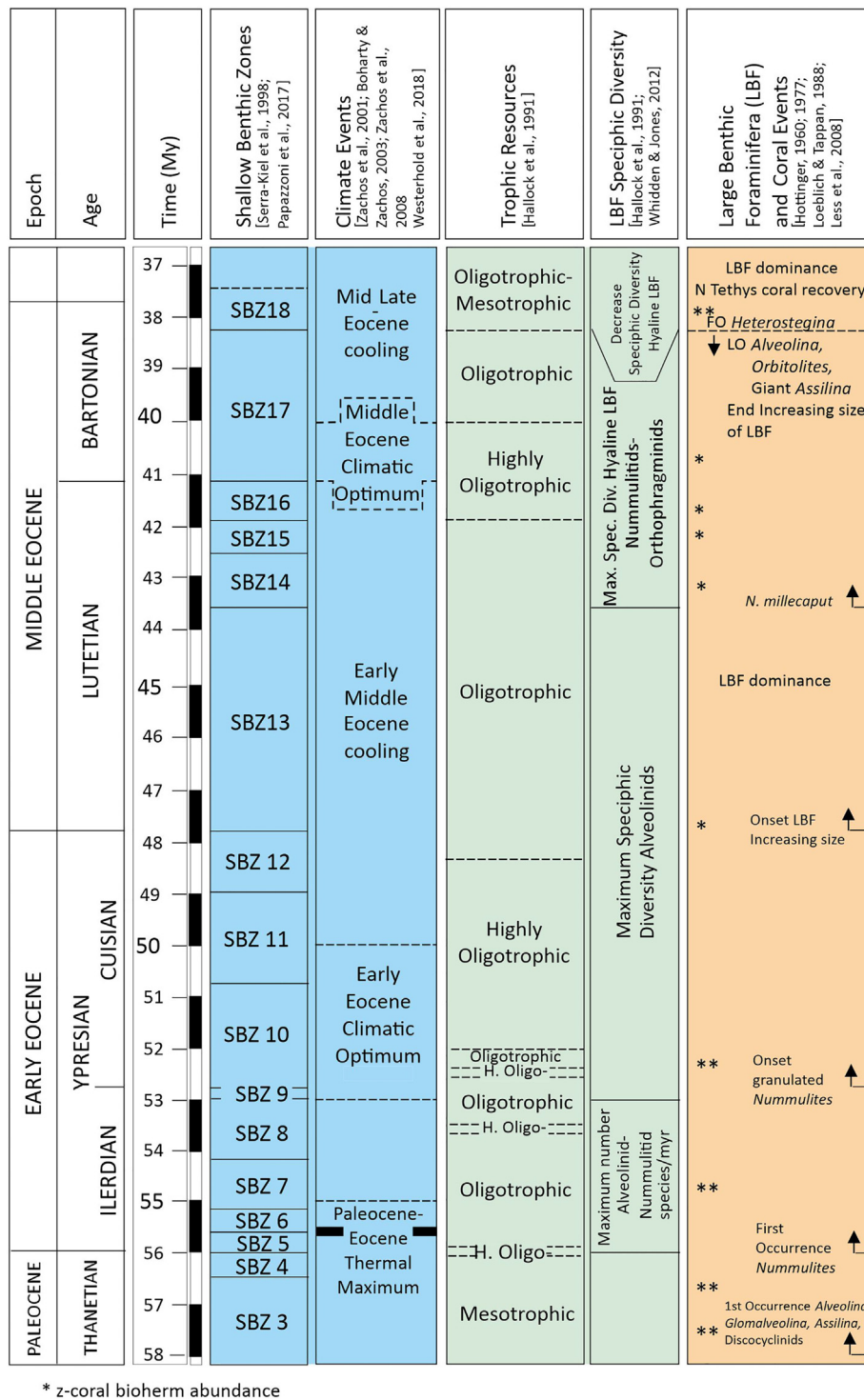
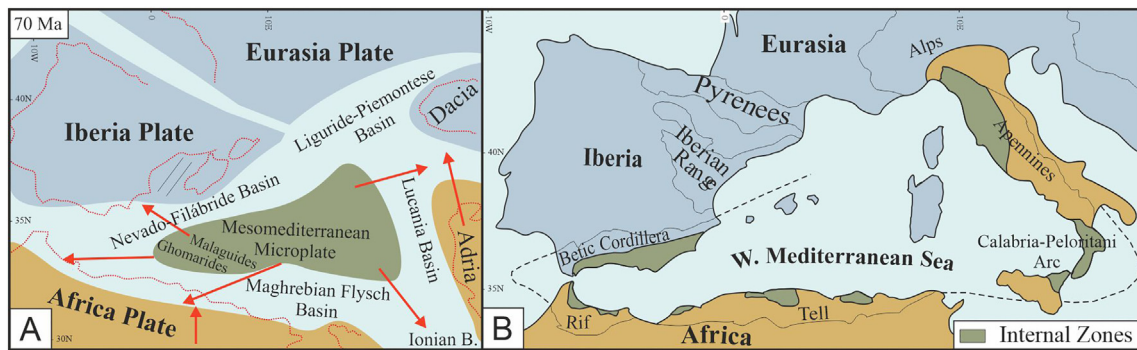


Fig. 1. Geological time chart showing the Eocene epochs, ages, numerical time scale, Shallow Benthic Zones (Shallow Benthic Zone), climatic events, trophic resources, larger benthic foraminifera diversity and larger benthic foraminifera and zooxanthellate coral events.

foraminifera by the rising of the calcite compensation depth level; (v) the diversification of many species of mammals, which moved towards previously inhospitable mid-high latitude areas; (vi) a large foraminiferal turnover; and (vii) the development of wide carbonate ramps in pericontinental mid-latitude areas and reef growth due to rising sea levels.

The study of the effects of Eocene warming is very important, as it provides insight into the effects of the current climate change, which is largely influenced by anthropogenic factors. Understanding the effects of Eocene warming could be a key to understanding the effects of the current climate change.

Nowadays, Eocene platform deposits are very widespread in the Mediterranean and neighbour sectors, which have been extensively studied (Scheibner and Speijer, 2008; and references therein): Spain, France, Italy, Turkey, Morocco, Algeria, Tunisia, Libya, Egypt, etc. These Eocene carbonate platforms were usually ramps rich in larger benthic foraminifera and zooxanthellate corals, developed mainly in two belts located on the margins of the Tethys Ocean. On the northern edge a carbonate belt developed at deduced latitudes of about 40°N, stretching from the Pyrenees to the Caucasus region, which included the Alpine, Adriatic, Apennine, Carpathian, Helenian and Anatolian platforms (Scheibner and Speijer,



**Fig. 2.** A) Palaeogeographic sketch map of the western Tethys for the Late Cretaceous period (70 Ma) with the location of the Mesomediterranean Microplate and the Ghomaride Domain. Red arrows indicate the tectonic movements during the Alpine orogeny. B) A geological sketch map of the Alpine chains in the central-western Mediterranean region with the location of the blocks (greenish colour) resulting from the Mesomediterranean Microplate.

2008; Pomar et al., 2017; Müller et al., 2019). The southern Tethyan margin was occupied by another carbonate belt, mostly below 25°N, now represented by North African countries from Morocco to Egypt and the Middle East (Scheibner and Speijer, 2008; Höntzsch et al., 2013; Pomar et al., 2017; Müller et al., 2019; Martín-Martín et al., 2020c).

The distribution of larger benthic foraminifera and zooxanthellate corals is controlled by climate and is restricted to a worldwide climatic gap with a minimum temperature of 15 °C–20 °C (Adams et al., 1990; Langer and Hottinger, 2000). The presence of either larger benthic foraminifera or corals is usually determined by water temperature, nutrient levels in water masses, terrestrial runoff and the presence or absence of upwelling currents (Herbig and Trappe, 1994; Scheibner and Speijer, 2008).

Recent palaeogeographic models of the western Tethys show that there were Eocene carbonate platforms in intermediate positions between these two main carbonate ramp belts in the margin of the Tethys, at approximately 30°N and between 0° and 10°E. These ramps developed on the southern margin of the Mesomediterranean Microplate (Fig. 2A), which was located in the westernmost Tethys in the transition to the Atlantic Ocean (Martín-Martín et al., 2020a, 2020b; Guerrero et al., 2021). Today, fragments of the Mesomediterranean Microplate are found in the alpine chains of the western-central Mediterranean (Fig. 2B). Studies performed recently in the Eocene platform from one of these fragments (Malaguide Domain, Internal Betic Cordillera, S Spain) (Fig. 2A) revealed that larger benthic foraminifera and zooxanthellate coral accumulations were more abundant than previously noted

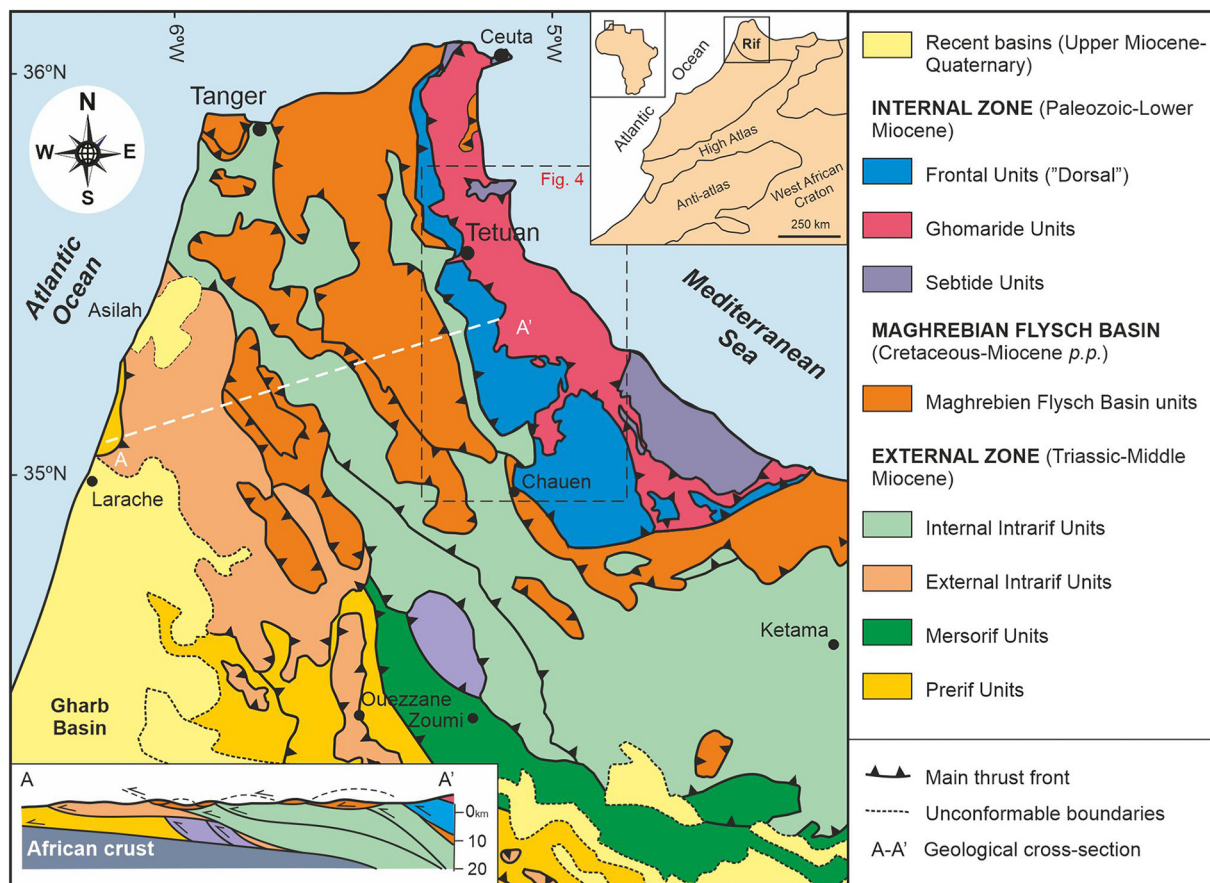


**Fig. 3.** The geological map and schematic geological cross-section of the western Rif Chain in northern Morocco, with the area's location depicted in Fig. 4. There is also an index map showing the main Moroccan chains in the upper right corner.

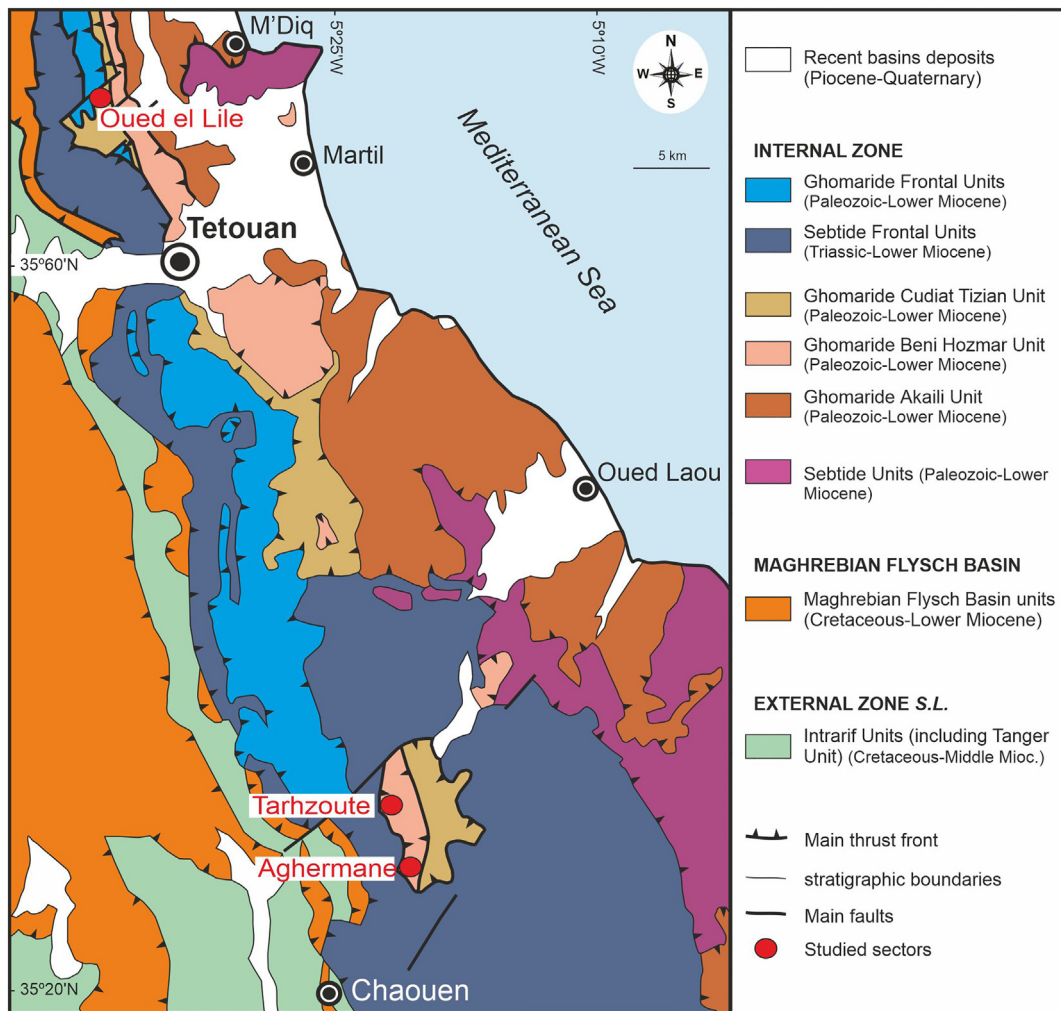


Fig. 4. The geological map of the area between Tetouan and Chaouen, with the location of the studied stratigraphic sections.

(Martín-Martín et al., 2020c, 2021; Tosquella et al., 2022; and references therein).

Another of these fragments was represented by the Ghomaride Domain (Fig. 2A), nowadays widespread in the Internal Rif Zone (northern Morocco) (Fig. 2B) (Doglioni, 1992; Martín-Martín et al., 2020a, 2020b; Guerrero et al., 2021; and references therein) and the aim of this work. This research presents the description and interpretation of micro- and macrofacies of three stratigraphic sections where the Eocene carbonate platform is well represented in the Ghomaride units. The performed study on the basis of the fossiliferous assemblage, texture and fabric, allowed reconstructing the depositional and palaeoenvironmental evolution of the Eocene platform (ramps-like) in this key-sector. The main trophic and photic conditions, as well as larger benthic foraminifera and coral events were also defined for the study area and correlated with the global ones. A comparison with the northern (Spain, Italy and Central Europe), intermediate (S, Spain), and southern (Moroccan Atlas, Algeria, Tunisia, Libya–Egypt and Middle East) above-mentioned Eocene platform belts from the Tethyan Domain was also performed. These correlations have revealed significant differences but also some coincidences, providing important constrains about the Eocene platform evolution at the Western Tethys scale.

## 2. Geological framework

The Rif Chain (Doglioni, 1992; Michard et al., 2002, 2008; Chalouan et al., 2008), along with the Betic Cordillera, constitutes the westernmost segment of the Alpine peri-Mediterranean mountain belts (Doglioni,

1992; Martín-Martín et al., 2020a, 2020b; Guerrero et al., 2021; and references therein) (Fig. 2B). This belt was formed through the fragmentation, drift and collision of the westernmost sector of the Mesomediterranean Microplate with the Africa Plate, involving the subduction of the Maghrebien Flysch Basin beneath the Mesomediterranean Microplate (Doglioni, 1992; Martín-Martín et al., 2020a, 2020b; Guerrero et al., 2021; and references therein) (Fig. 2A). The Ghomaride fragment of the Mesomediterranean Microplate became the Internal Rif Zone, whilst the North Africa Margin is represented by the External Rif Zone (Chalouan and Michard, 2004; Frizon de Lamotte et al., 2017; Michard et al., 2017; Leprêtre et al., 2018) (Fig. 3). The Maghrebien Flysch Basin units (Fig. 3), which are prevalently involved in subduction, are sandwiched between the Internal and External Rif Zones (Chalouan and Michard, 2004; Chalouan et al., 2008; Michard et al., 2008).

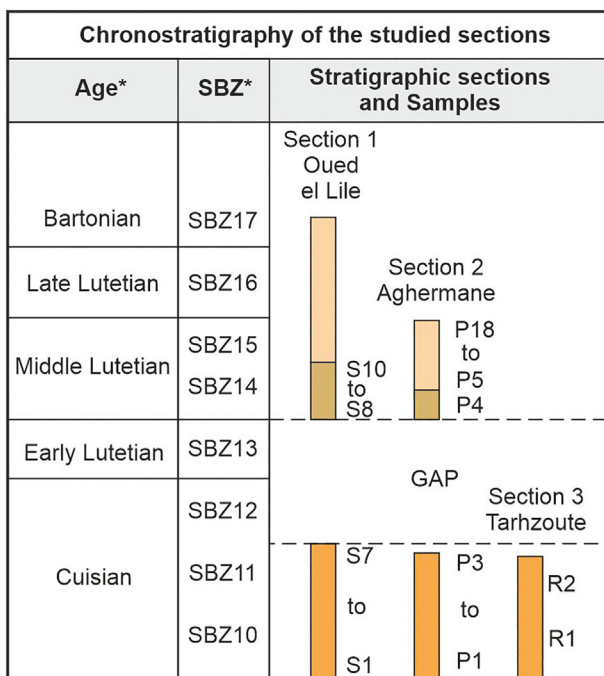
The Internal Rif Zone (Fig. 3) consists of the Sebtide, Ghomaride and Frontal units (tectonic elements unrooted from the Sebtide and Ghomaride units), arranged from bottom to top (Maaté, 1984; Martín-Algarra, 1987; Jabaloy-Sánchez et al., 2019). The Ghomaride Complex (Maaté, 1984) consists of a basement that is minimally affected by Variscan metamorphism and includes Palaeozoic slates, greywackes, limestones and siliceous beds. This is followed by unconformable Triassic continental redbeds and shallow carbonates. The succession continues with clear stratigraphic continuity to Jurassic carbonate platform deposits and Cretaceous deep-water deposits arranged in a transgressive sequence. The succession is completed by shallow to deep marine Cenozoic deposits (Maaté et al., 2000; Hlila et al., 2007), which usually outcrop in small, discontinuous and highly deformed slices.

The study focuses on the Ghomaride and the Internal Frontal units of Ghomaride origin, located between Tetouan and Chaouen in the Moroccan Internal Rif Zone (Fig. 4). In detail, three Eocene stratigraphic sections have been studied in the areas of Oued el Lile, Aghermame and Tarhzoute (Fig. 4). Shallow Benthic Zones (SBZ) of larger benthic foraminifera (*sensu* Serra-Kiel et al., 1998a, 1998b) have been recognised to establish the age of the sections. The studied period includes Shallow Benthic Zones 10 to 17.

The Oued el Lile section is part of the Belouazene Unit (Raoult, 1966), which belongs to the Ghomaride Frontal Units. The reconstructed succession consists of 60 m of bioclastic limestones from the Lower Eocene and 60 m of yellowish marls and calcareous sandstones from the middle Eocene. The lowermost Eocene succession includes the Cuisian (represented by Shallow Benthic Zone 10 and Shallow Benthic Zone 11 in Fig. 5) (Maaté, 1996; Maaté et al., 2000). After a stratigraphic gap extending from the late Cuisian to the early Lutetian, the middle Eocene succession is well represented (Shallow Benthic Zones 14 to 17; Maaté et al., 2000). The above-mentioned gap is recognised in other western Tethys sectors (Martín-Martín et al., 2020c, 2021; Tosquella et al., 2022) having a regional meaning related to a shallowing period with emersion and/or erosion.

The Aghermame section belongs to the Ghomaride Beni Hozmar Unit (Chalouan, 1986). The Eocene succession comprises 40-m-thick organogenic Ghomaride limestones (from the lower–middle Eocene *p.p.*) and 40 m of yellowish marls and calcareous sandstones from the middle Eocene *p.p.*. The lower Eocene is represented by the Cuisian Shallow Benthic Zones 10–11 (Fig. 5 adapted from Hlila et al., 2007). After a gap that extends from the late Cuisian to early Lutetian, the middle Eocene is represented by the middle Lutetian Shallow Benthic Zones 14–15 (according to Hlila et al., 2007).

The Tarhzoute section also belongs to the Ghomaride Beni Hozmar Unit (Chalouan, 1986). In this section, the Eocene succession is made up of 20 m of lower Eocene organogenic limestone, which represents the Cuisian Shallow Benthic Zones 10–11 (Fig. 5) (Hlila et al., 2007).



\* According to Maaté et al. (2000) and Hlila et al. (2007); SBZ = Shallow Bentic Zone (Serra-Kiel et al., 1998 a,b)

### 3. Materials and method

The main approach involves field observations, the structural analysis and tectonic controls, reconstruction of the stratigraphic record and examination of lithological and sedimentological features. Field data is supplemented by laboratory analyses, which primarily focus on defining the fossil content, particularly for larger benthic foraminifera and zooxanthellate corals that are abundant at various stratigraphic levels. During fieldwork, the main litho- and biofacies were recognised and described (as listed in Table 1) with the goal of understanding their relationship to sedimentary evolution; whilst for the stratigraphic terminology Owen (2009) was followed.

**Table 1**  
The lithostratigraphic data of the study stratigraphic sections (Logs).

Thickness (m)	Samples	Age	Field lithofacies
<i>Stratigraphic section 1 (Log 1) – locality: Oued El Lile (Sedimentary cover of Ghomaride Frontal Units) (Oued el Lile Formation)</i>			
25		Bartonian to Lutetian	A13 (Lateral-superior lithofacies than A1): Sandy brownish–ochraceous marls with decimetric (up to 50 cm thick) brownish arenitic bed intercalations
35	S10-S8-S9		A12: Alternating pelites and detrital limestones with glauconite grains and frequent Nummulites (0.5–1 cm), discocycline (0.5–2 cm), algae, and levels of Assilina and Solenomeris.
Unconformity			
10	S7	Cuisian	A3: Limestones with abundant little Nummulites and occasional lamellibranchs (3–4 cm), and algae
20	S6-S5-S4		A2: Limestones with abundant Assilina and Solenomeris
29	S2-S3		A11: Homogeneous metric greyish micritic limestone beds with rounded quartz, and a few millimetric Nummulites
1	S1		A1: stratified light brown pelitic–marly–calcareous succession with frequent slumps; the marly–pelitic portion accounts for 80 %; the limestones and/or calcareous-marls accounts for 20 %
Unconformity			
0.2	–	Jurassic	Discontinuous oxidised (Fe oxides) <i>hard ground</i> at the top of Jurassic Limestones
40			Micritic limestones with chert, algae and benthic foraminifera
<i>Stratigraphic section 2 (Log 2) – locality: Aghermame (Ghomaride sedimentary cover) (Oued el Lile Formation)</i>			
>50			Not exposed
35	P18 to P5	Lutetian	A10: Brownish marls with discontinuous limestones beds with large Nummulites (>2 cm) and algae
5	–		AA: Fine limestones
15	P4		A9: Algae limestones
3	–		A8: Conglomeratic marker-bed corresponding to the marker-bed recognised at the base of the Malvariche Fm
4	–		A7: Limestones with algae, abundant large sized and flat-shaped Nummulites (up to 2 cm), colonised by Solenomeris and Assilina and occasional Lamellibranchs (3–4 cm)
Unconformity			
3	P3	Cuisian	A3: Limestones with abundant little Nummulites and occasional lamellibranchs (3–4 cm)
–	–		A: decimetric beds of alveoline-rich (up to 2 cm) limestones (Nummulites are absent)

Fig. 5. A biostratigraphic framework of the Eocene Ghomarides in the study area.

Table 1 (continued)

Thickness (m)	Samples	Age	Field lithofacies
2	P2		A2: Limestones with abundant <i>Assilina</i> and <i>Solenomeris</i>
1	P1		A: Decimetric beds of Alveoline-rich (up to 2 cm) limestones ( <i>Nummulites</i> are absent)
Unconformity >100		Triassic	Red pelites with conglomerates
Stratigraphic section 3 (Log 3) – locality: Tarhzoute (Ghomaride sedimentary cover) (Oued el Lile Formation)			
Tectonic contact			
3		Cuisian	A5: Limestones with <i>Assilina</i> and <i>Solenomeris</i>
2			A7: Limestones with algae, large sized and flat shaped (up to 2 cm) <i>Nummulites</i> colonised by <i>Solenomeris</i> , and <i>Assilina</i>
1			A5: Limestones with <i>Assilina</i> and <i>Solenomeris</i>
4			A3: Limestones with abundant little <i>Nummulite</i> and occasional lamellibranchs (size 3–4 cm)
1	R2		A4: Limestones with <i>Discocyclus</i>
3	R1		A6: Limestones with <i>Discocyclus</i> , <i>Assilina</i> , medium-sized <i>Nummulites</i> and red algae
3			A5: Limestones with <i>Assilina</i> and <i>Solenomeris</i>
1			A3: Limestones with abundant little <i>Nummulite</i> and occasional lamellibranchs (size 3–4 cm)
			A2: Limestones with abundant <i>Assilina</i> and <i>Solenomeris</i>
Unconformity >50		Triassic	Red pelites with conglomerates

In particular, three Eocene stratigraphic sections have been studied, measured and sampled (Fig. 4). Thirty samples were collected to maximise the number of different biofacies in the field (10 from Oued el Lile, 18 from Aghermene and 2 from Tarhzoute). These samples were then prepared for microfacies analysis in thin sections (2.0 × 3.0 cm) as illustrated in Fig. 5. An optical microscope (Nikon Eclipse E 200) was used to analyse the sedimentological and micropalaeontological features of the samples. Microfacies analysis and lithology description are made following the methodology of Flügel (2010) whilst the microfacies terminology has been referred to Embry and Klovan (1971). The identification of larger foraminifera was performed following the method of Loeblich and Tappan (1988). In this study, the genus *Assilina* includes both *Assilina* s.s. and ‘operculiniform *Assilina*’ as defined by Tosquella and Serra-Kiel (1998). Photographs were taken with a digital camera (Nikon DS-Fi2), transferred to a PC using Nikon’s Digital Sight DS-U3 microscope camera controller and processed using the microscope imaging software Nikon NIS Elements F4.

## 4. Results

### 4.1. Lithostratigraphy

The analysed successions represent the Eocene sedimentary cover of the Ghomaride Unit and the Frontal Units with Ghomaride origins (Rif, Chain). Three selected stratigraphic sections have been studied (Figs. 5–7): Log 1 (Oued El Lile locality, thickness 120 m, 10 samples), Log 2 (Aghermene locality, thickness 80 m, 18 samples) and Log 3 (Tarhzoute locality, thickness 20 m, two samples), located in the Talassemiane National Park area (east of Chefchaouen). These successions belong to the informally defined Oued el Lile Formation (Perri et al., 2022) and can be considered part of the Xiquena Group established for the entire Betic–Rif Cordillera (Martín-Algarra, 1987).

#### 4.1.1. Stratigraphic section 1/Log 1 (Oued El Lile, 36/721753E/553002N UTM coordinates; thickness 120 m) (Fig. 7A)

The Eocene succession (Maaté, 1996; Maaté et al., 2000) rests on Jurassic limestones (micritic limestones with chert, algae and benthic foraminifera) through an unconformity (stratigraphic gap of over 90 Ma) and it is composed of different lithofacies associations. In the Eocene succession, two main stratigraphic intervals have been recognised, separated by an unconformity (gap of approximately 2–3 Ma; Fig. 5). The lower interval shows four main lithofacies (A1, A11, A2, A3), whilst the upper one is characterised by only two lithofacies (A12 and A13). All lithofacies are described synthetically in Table 1 and are shown in Figs. 5–7. The lower interval is composed by 1 m of stratified light brown pelitic–marly–calcareous beds (lithofacies A1) with frequent slumps (marly–pelitic 80 %; limestones–calcareous 20 %), 29 m of homogeneous metric greyish micritic limestone beds with rounded quartz, and a few millimetric *Nummulites* (lithofacies A11), 20 m of limestones with abundant *Alveolina* (Fig. 7D), *Assilina* and *Solenomeris* (lithofacies A2) and 10 m of limestones with abundant little *Nummulites* and occasional lamellibranchs (3–4 cm), and algae (lithofacies A3). The whole interval shows gradual transitions among the different lithofacies. After an unconformity with associate gap, the second interval is found. It is made up of 35 m of alternating pelites and detrital limestones with glauconite grains and bioclastic content with medium-size larger benthic foraminifera (lithofacies A12), and 25 m of sandy brownish–ochraceous marls with decimetric (up to 50 cm thick) brownish arenitic bed intercalations (lithofacies A13). This second interval also shows gradual transitions between the two lithofacies. The absence of flat-shaped larger benthic foraminifera suggests a more proximal situation with respect to the other two studied sections.

#### 4.1.2. Stratigraphic section 2/Log 2 (Aghermene, 36/721753E/553002N UTM coordinates; thickness 80 m) (Fig. 7B)

The Eocene succession (Hilila et al., 2007) rests on Triassic red beds (red pelites with conglomerates) through an unconformity (gap of over 145 Ma; Fig. 5). The succession shows two main stratigraphic intervals, separated by the same unconformity previously described (Log 1). In the lower interval, an assemblage of three main lithofacies (A, A2, A3) has been recognised. The lithofacies, especially the highest one (A3), show similar characteristics to those in the previous log. The upper interval contains four lithofacies (A7, A8, A9 and A10). All lithofacies are described synthetically in Table 1 and are shown in Figs. 5–7. The lower interval is made up of 3 m of limestones with abundant *Assilina* and *Solenomeris* (lithofacies A2), <1 m of decimetric beds of small-size alveoline-rich (up to 2 cm) limestones (lithofacies A) (Fig. 7E), and limestones with abundant little *Nummulites* and occasional lamellibranchs (lithofacies A3). After an unconformity with associate gap, the second interval appears made of 4 m of algal–solenomeris limestones (lithofacies A7) with abundant large sized lenticular- and flat-shaped larger benthic foraminifera (Fig. 7F) and occasional lamellibranchs (3–4 cm), 3 m of a conglomeratic bed (lithofacies A8), 15 m of algal limestones (lithofacies A9), 5 m of fine limestones (lithofacies AA), and 35 m of brownish marls with discontinuous limestone beds with large *Nummulites* (>2 cm) and algae (lithofacies A10). The presence of flat-shaped larger benthic foraminifera suggests a more distal position with respect to section 1.

#### 4.1.3. Stratigraphic section 3/Log 3 (Tarhzoute, 36/721753E/553002N UTM coordinates; thickness 20 m) (Fig. 7C)

This section is characterised by a more reduced succession (Hilila et al., 2007), which is correlatable with the lower interval of the two previously described logs and contains an assemblage of six lithofacies (A2, A3, A4, A5, A6 and A7), which partially correspond to those in the other logs. All lithofacies are described synthetically in Table 1 and are shown in Figs. 5–7.

This unique interval is composed of <1 m of limestones with abundant *Assilina* and *Solenomeris* (lithofacies A2), 1 m of limestones with

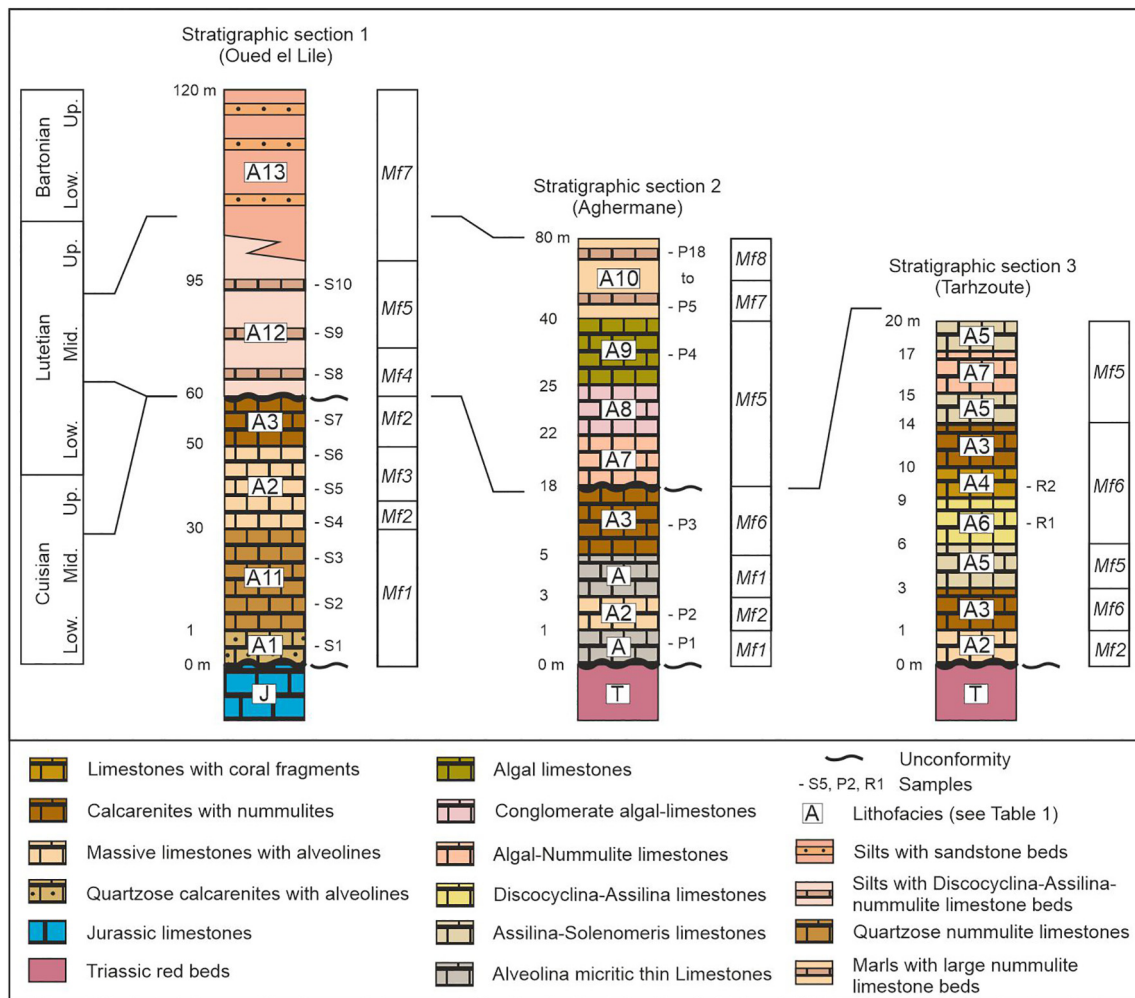


**Fig. 6.** The studied stratigraphic sections represented as columns. The sections are not in the same scale due to the difference in thickness between section 3 and the others. The figure also displays the distribution of the defined lithofacies and microfacies (Mf1 to Mf8) and the location of the studied samples.

abundant little Nummulite and occasional 3–4 cm-size lamellibranchs (lithofacies A3), 3 m of limestones with Assilina and Solenomeris (lithofacies A5), 1 m of limestones with medium-sized - flat-shaped larger benthic foraminifera and red algae (lithofacies A6), 1 m of limestones with Discocyclusina (lithofacies A4), 4 m of limestones with abundant little Nummulite and occasional 3–4 cm-size lamellibranchs (lithofacies A3), 2 m of algal limestones (Fig. 7G) and large sized lenticular- and flat-shaped (up to 2 cm) larger benthic foraminifera (lithofacies A7) (Fig. 7H), and 3 m of limestones with Assilina and Solenomeris (lithofacies A5). The presence of flat-shaped larger benthic foraminifera suggests equivalent proximal–distal situation than section 2 and a more distal position with respect to section 1.

Despite the slightly different thicknesses, all the examined successions are well correlated laterally, both in terms of age and many lithofacies. In this way, lithofacies A3 has been recognised in all logs. It is located at the top of the lower interval (just below the unconformity surface) in sections 1 and 2 (Fig. 5). This lithofacies could represent a local marker bed for a larger area.

#### 4.2. Microfacies description

Eight microfacies (Mf1 to Mf8) have been identified with unequal occurrence in the studied sections (Figs. 8 and 9; Table 2).

##### 4.2.1. Mf1 - quartz-rich calcarenites with larger benthic foraminifera packstone (Fig. 8A)

This microfacies, ranging from poorly to moderately sorted, is composed of abundant rounded fine to medium quartz grains (20 %–25 %) and a diverse biotic assemblage dominated by larger benthic foraminifera. The main components, as shown in Fig. 9, are *Nummulites* (25 %), *Alveolina* (5 %–15 %), *Discocyclusina* (5 %–10 %), rotaliids (5 %–10 %), *Assilina* and operculiniform *Assilina* (3 %–10 %), *Amphistegina* (3 %–10 %), and textulariids (3 %–5 %) in an echinoid debris-rich matrix (10 %–15 %). Other common components include bivalve molluscs (2 %–3 %), bryozoans (2 %–3 %), rodophycean (2 %–3 %) and acervulinid remains (2 %–3 %). Discorbids, annelids and small benthic and planktic foraminifera are occasionally observed. This microfacies is present at the base of stratigraphic section 1 (Oued el Lile) with a thickness of 29 m (lithofacies A1 and A11) and in the lower part of stratigraphic section 2 (Aghermame) in two intervals with thicknesses of 1 and 2 m, respectively (lithofacies A).

##### 4.2.2. Mf2 - hyaline larger benthic foraminifera-rich coral–foralgal rudstone (Fig. 8B)

This poor-sorted microfacies consists of a significant amount of grains and small cobbles (Fig. 9) from colonial corals (5 %–10 %), *Sporolithon* rhodolith (10 %–20 %) and *Solenomeris* macroid (10 %–15 %) structures, which are sometimes wrapped by *Acervulina linearis* (5 %) specimens in

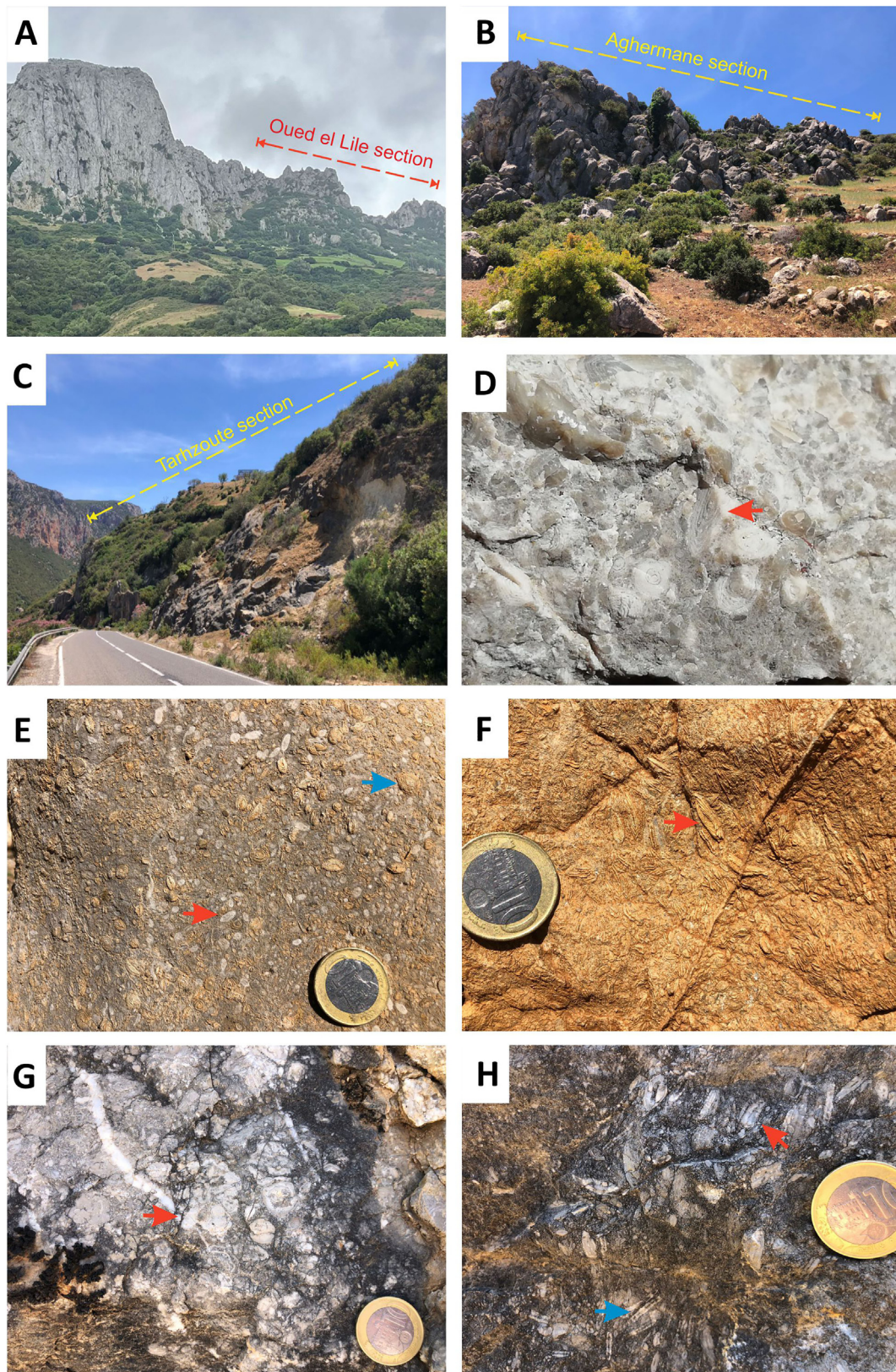


**Fig. 7.** Photomosaic of the studied Ghomaride stratigraphic sections and field lithofacies: A) Oued el Lile section panoramic view; B) Aghermene section panoramic view; C) Tarhzoute section panoramic view; D) Alveolina limestones from the Oued el Lile section; E) limestone rich in small alveolines (red arrow) and nummulites (blue arrow) from Aghermene section; F) large-sized lenticular-shaped hyaline larger benthic foraminifera from Aghermene section; G) algal limestone (rhodoliths) from Tarhzoute section; H) large-sized lenticular- (red arrow) and flat-shaped (blue arrow) hyaline larger benthic foraminifera from Tarhzoute section.

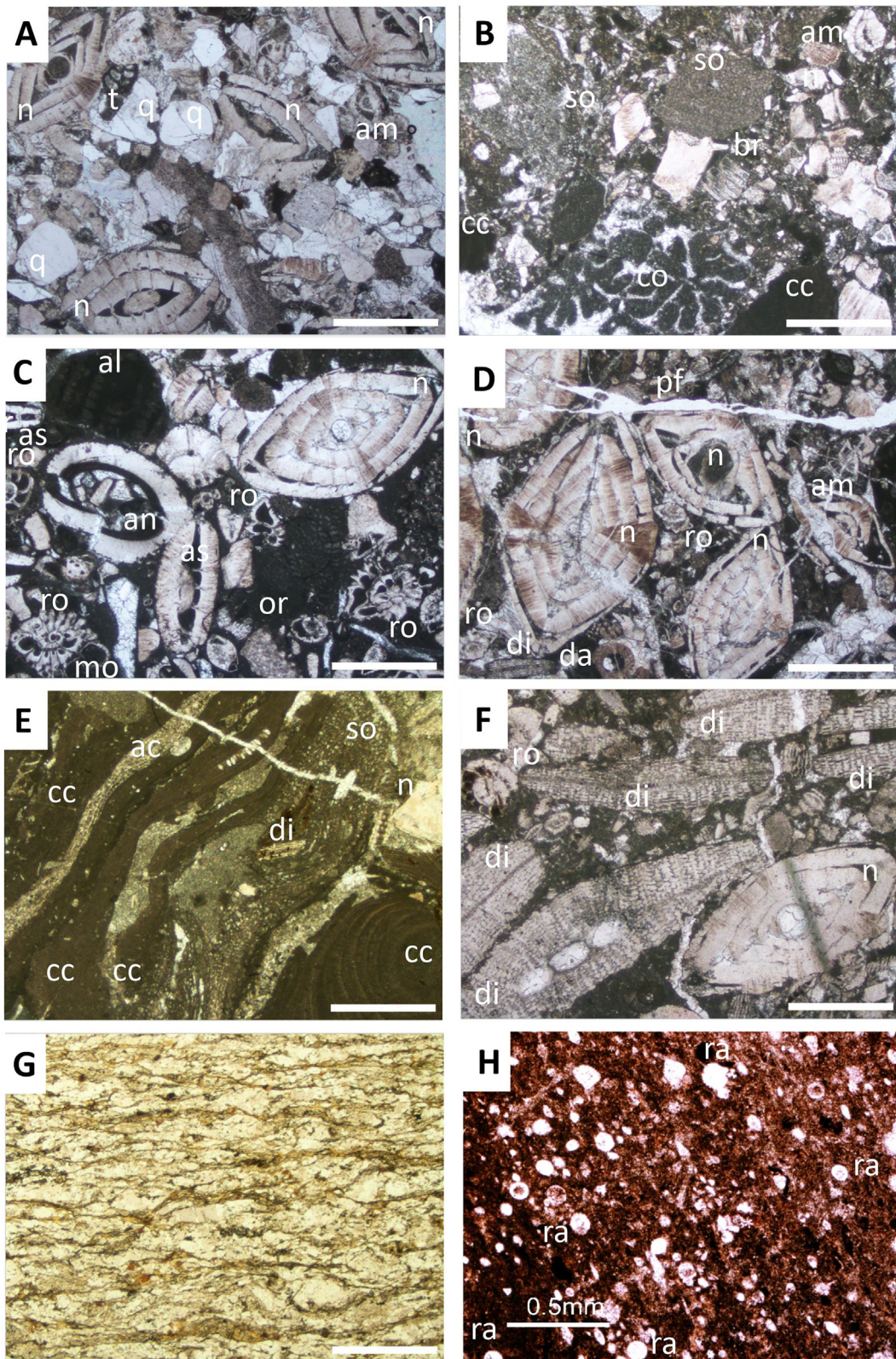


**Fig. 8.** Photomicrographs of microfacies of the Ghomaride stratigraphic sections: A) *Mf1*, sample S-2 (10); B) *Mf2*, sample S-7 (17); C) *Mf3*, sample S-5 (19); D) *Mf4*, sample S-8 (7); E) *Mf5*, sample PNT-4 (2); F) *Mf6*, sample R-2 (9); G) *Mf7*, sample PNT-5 (1); H) *Mf8*, sample PNT-16 (PNT-2018). Scale bar: A–G, 1 mm; H, 0.5 mm. Key: ac, acervulinid; al, alveolina; am, amphistegina; an, annelid; as, assilina; br, bryozoan; cc, crustose coralline algae; co, coral; di, discocyclina; da, dasycladacean algae; ed, echinoid debris; mo, mollusc; n, nummulites; or, orbitolites; pf, planktic foraminifer; q, quartz; ra, radiolarian; ro, rotaliid; so, solenomerid; t, textulariid.

a hyaline larger benthic foraminifera-rich packstone matrix. The main matrix fossil content includes abundant *Discocyclina* tests (15%–25%), *Nummulites* (10%–20%), rotaliids (10%), *Assilina* (5%–10%),

*Amphistegina* (5%–10%) and echinoid debris (5%–15%). Other common components include bryozoans (2%–3%), textulariids (2%–3%) and small benthic and planktic foraminifers (2%–3%). Ostracods and

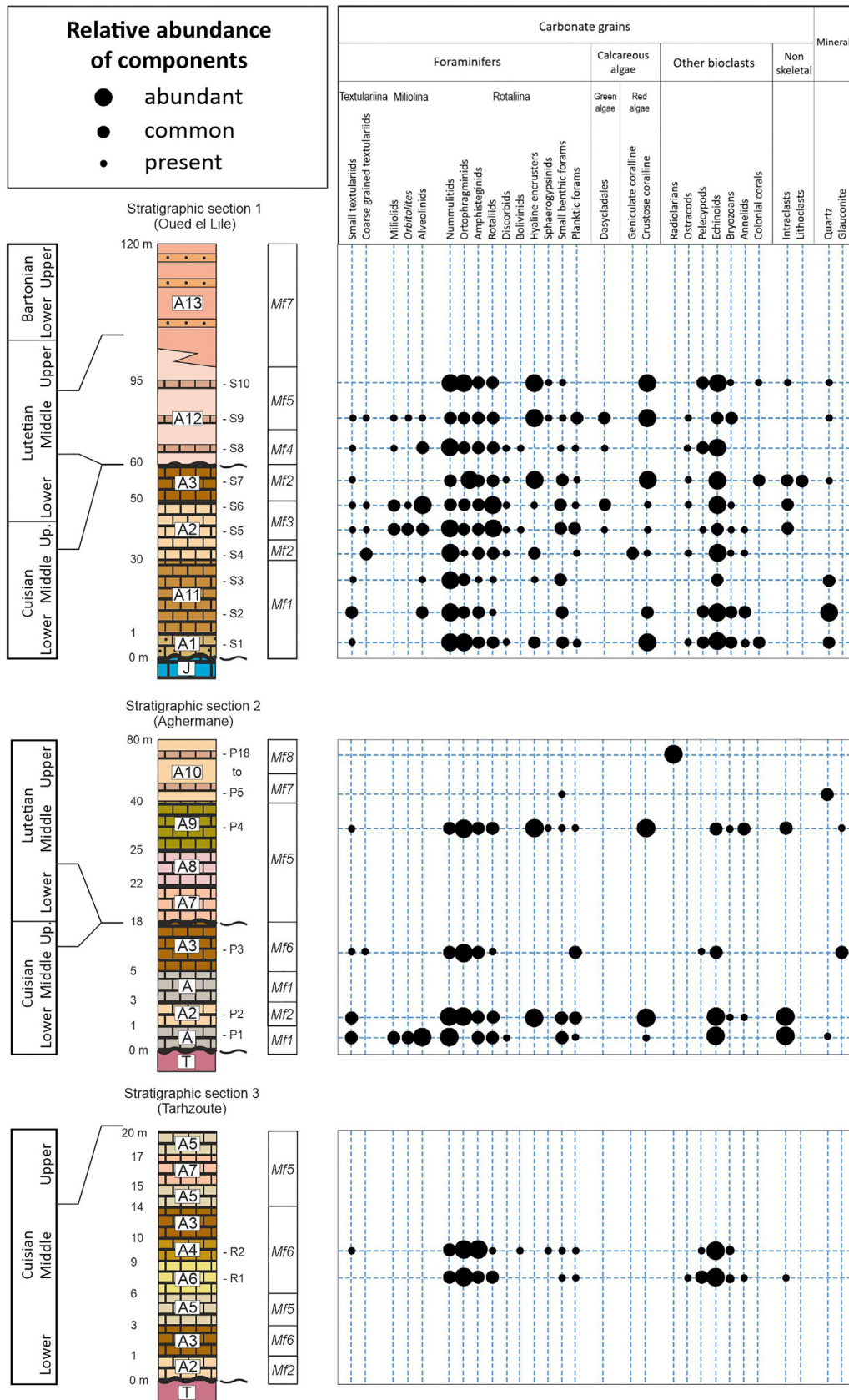


**Fig. 9.** The relative abundance of components in the studied thin sections from the three stratigraphic sections. The components are categorised into three groups based on the estimated relative abundance under the optical microscope: (1) present is used when the element is seen at least once in the whole thin-section; (2) common is used when the element appears at least once using an objective  $\times 4$ ; (3) abundant is used when the element appears 2 to 4 times using an objective  $\times 4$ .

**Table 2**  
The upper Ypresian to middle Lutetian litho-microfacies recorded in the Cenozoic sedimentary cover of the Ghomaride Complex.

Microfacies (Mf1 to Mf8)	Samples	Description	Fossils and non-skeletal grains common and/or abundant*	Fossils and non-skeletal grains present and/or rare	Depositional environment
Mf1	S-1 S-2 S-3 P-1	Quartz-rich calcarenites with LBF packstone	Alveolina*, Nummulites*, Discocyclina, Assilina, operculiniform Assilina, Amphistegina, rotaliids, textulariids; crustose coralline and acervulinid remains; pelecypods; bryozoans; echinoid spines and plates*; quartz*	Discorbids, annelids, unspecific small benthic and planktic foraminifers	'Transgressive reworked deposit' in inner ramp Upper subtidal Euphotic environment
Mf2	S-4 S-7 P-2	Hyaline LBF-rich coral–foralgal rudstone	Nummulites*, Assilina, Amphistegina, rotaliids, textulariids, unspecific small benthic and planktic foraminifers, Solenomeris macrooids* and other acervulinids; colonial corals; Sporeolithon rhodoliths*, geniculate coralline remains; bryozoans; echinoid debris*; intraclasts	Discorbids, ostracods	Middle ramp maërl Mesophotic environment
Mf3	S-5 S-6	Porcelaneous LBF and rotaliid-rich packstone–grainstone	Alveolina*, Orbitolites, Nummulites, Assilina, Discocyclina, Amphistegina, rotaliids*, miliolids; rhodophycean and solenomerid remains; dasyclade algae ( <i>Ovulites?</i> ); echinoid spines and plates	Discorbids, textulariids, unspecific small benthic and planktic foraminifers; bryozoans; ostracods	Inner ramp sea-grass Euphotic environment
Mf4	S-8	Nummulite packstone	Nummulites*, Alveolina, Assilina, operculiniform Assilina, Discocyclina, Amphistegina, rotaliids, textulariids and other small benthic foraminifers; dasyclade algae; mollusc remains; echinoid spines and plates	Miliolids, discorbids, bolivinids, planktic foraminifers; ostracods	Middle ramp LBF accumulations (nummulitids) Mesophotic environment
Mf5	S-9 S-10 P-4	Hyaline LBF-rich coral–foralgal boundstone	Nummulites*, Assilina, Discocyclina*, Amphistegina, hyaline encrusting foraminifers (acervulinid, planorbulinids); rhodoliths*; colonial corals; ostreids; bryozoans; echinoid spines and plates; quartz	Rotaliids, textulariids, unspecific small benthic foraminifers; ostracods	Distal middle ramp maërl Mesophotic environment
Mf6	R-1 R-2 P-3	Discocycline packstone	Discocyclina*, Amphistegina*, Nummulites, Assilina, rotaliids, planktic foraminifers; bivalve mollusc remains; echinoid debris	Sphaerogyp-sina, bolivinids, textulariids, unspecific small benthic and planktic foraminifers; bryozoans; ostracods; glauconite	Distal middle ramp LBF accumulations (ortophragminids) Mesophotic environment Outer ramp (circalittoral) Oligophotic environment Slope Aphotic environment
Mf7	P-5 to P-15	Azoic quartzsiltite	Fine-sized quartz grains		
Mf8	P16 to P-18	Marlysiltitic wackestone with radiolarians	Spumellarid radiolarians		

discorbids appear only occasionally. This microfacies is present in three stratigraphic sections. It appears in the lower part (lithofacies A2 and A3) of stratigraphic section 1 (Oued el Lile) in two intervals with thicknesses of 5 and 10 m, respectively. This microfacies also appears in the lower part (lithofacies A2 and A3). It also can be found in the lower part of stratigraphic section 2 (Aghermane) in a 2 m thick interval (lithofacies A2) and at the base of stratigraphic section 3 (Tarhzoute) in a 1-m thick interval (lithofacies A2).

#### 4.2.3. Mf3 - porcelaneous larger benthic foraminifera and rotaliid-rich packstone–grainstone (Fig. 8C)

This microfacies, ranging from moderate to well sorted, has a main fossil association (Fig. 9) composed of *Alveolina* (15%–20%) and rotaliid (15%–20%) tests, sometimes represented as rounded reworked grains. *Nummulites* (10%–15%), echinoid spines and plates (10%–15%) are also frequent. Common components in the microfacies include *Orbitolites* (5%–10%), miliolids (5%–10%), *Assilina* (5%–10%), *Discocyclina* (5%–10%) and *Amphistegina* (5%–10%) as well as rhodophycean and solenomerid remains (5%–10%). Rare to frequent components include dasyclade algae (2%–3%) and discorbids, textulariids, bryozoans, ostracods and small benthic and planktic foraminifers are only present occasionally. This microfacies is found only in the lower part of stratigraphic section 1 (Oued el Lile) with a thickness of 15 m (lithofacies A2).

#### 4.2.4. Mf4 - Nummulite packstone

This microfacies (Fig. 8D) is a poorly to moderately sorted microfacies composed mainly (Fig. 9) of abundant tests of *Nummulites* (25%–30%) and echinoid plates and spines (15%). Other important components include *Alveolina* (10%–15%), *Assilina* and operculiniform *Assilina* (10%–

15%), *Discocyclina* (10%–15%), rotaliids (10%–15%) and *Amphistegina* (5%–10%). In lesser amounts, molluscs (5%), dasyclade algae (2%–3%), miliolids (2%–3%), discorbids (2%–3%), textulariids (2%–3%) and small benthic foraminifers (2%–3%) are also present. Isolated ostracods, planktic foraminifers and bolivinids appear only occasionally. This microfacies is found only in the intermediate part of stratigraphic section 1 (Oued el Lile) with a thickness of 10 m (lithofacies A12).

#### 4.2.5. Mf5 - hyaline larger benthic foraminifera-rich coral–foralgal boundstone (Fig. 8E)

This microfacies (Fig. 8E) is a poorly to moderately sorted microfacies with a boundstone to packstone texture (Fig. 9). It is abundant in warty-to-lumpy rhodoliths and coralline fruticose structures (20%–30%) often encrusted with hyaline foraminifers (5%–10%) from the acervulinid/planorbulinid groups. Genera such as *Sporolithon* and *Lithothamnion* are recognised in the construction of rhodoliths and non-specific rhodophyceans have also been observed to form lamellar growths encrusted by thin sheets of *Acervulina linearis*. Ostreid and coral remains sometimes form the inner core of rhodoliths ('encrusting' sensu Woelkerling et al., 1993). *Solenomeris* (5%–15%) is also common, arranged in multilayered successions with rhodophycean algae and encrusting foraminifers to form rhodolith/macroid structures. A large part of the matrix is made up of abundant hyaline larger benthic foraminifera, among which *Nummulites* (15%–25%), *Discocyclina* (15%–25%), *Amphistegina* (10%) and *Assilina* (2%–3%) are the main representatives. Other common components include echinoid spines and plates (10%), ostreids (5%–10%), bryozoans (5%), corals (5%) and scattered rounded quartz grains (5%). Occasionally, rotaliids, textulariids, ostracods, small benthic and planktic foraminifers have also been observed in the fine fraction of the calcarenite matrix. This

microfacies is present in all three stratigraphic sections under study. It is recognisable in the upper part of stratigraphic section 1 (Oued el Lile) with a thickness of 20 m (lithofacies A12). It also appears in the intermediate part of stratigraphic section 2 (Aghermame) with a thickness of 22 m (lithofacies A7, A8 and A9). In stratigraphic section 3 (Tarhzoute), this microfacies characterises two beds in the intermediate and upper parts of the section, which have a thickness of 3 m and 6 m, respectively (lithofacies A5 and A7).

#### 4.2.6. *Mf6 - discocyline packstone (Fig. 8F)*

This microfacies is poorly to moderately sorted and mainly (Fig. 9) composed of abundant tests of *Discocyclus* (25%–35%), *Amphistegina* (15%–20%), *Nummulites* (10%–15%) and, to a lesser extent, echinoid debris (5%–10%), bivalve mollusc remains (5%), *Assilina* (5%), rotaliids (2%–3%) and planktic foraminifers (1%–2%). Tests of *Sphaerogypsina*, bryozoans, ostracods, textulariids, bolivinids and other unspecific small benthic foraminifers appear only occasionally in the matrix. The presence of scattered glauconite, mainly filling the chambers of some foraminifers, has also been observed. This microfacies is present in the intermediate part of stratigraphic section 2, where it shows a thickness of 13 m (lithofacies A3) and at two beds in the lower and intermediate parts of stratigraphic section 3 (Tarhzoute) with a thickness of 2 and 6 m, respectively (lithofacies A3, A4 and A6).

#### 4.2.7. *Mf7 - azoic quartzsiltite (Fig. 8G)*

This microfacies is poorly to moderately sorted and shows a significant presence of rounded fine-sized quartz grains. It appears highly altered and is affected by tectonic processes (Fig. 9). No fossil remains have been observed in this microfacies, although planktonic foraminifera are found in the levigates. This microfacies occurs at the top of stratigraphic section 1 (Oued el Lile), where it shows a thickness of 20 m (lithofacies A13) and at the upper part of stratigraphic section 2 (Aghermame) with a thickness of 20 m (lithofacies A10).

#### 4.2.8. *Mf8 - marly-siltitic wackestone with radiolarians (Fig. 8H)*

This microfacies is moderately sorted with a wackestone texture showing numerous spherical specimens of spumellarid radiolarians (Fig. 9). In the levigates, planktonic foraminifera is also found. This

microfacies is present only at the top of stratigraphic section 2 (Aghermame) with a thickness of 20 m (lithofacies A10).

## 5. Discussion

### 5.1. Depositional environment interpretation

The palaeoenvironmental interpretation is predominantly based on the main litho- and microfacies. Although the recognised microfacies are found in three different stratigraphic sections, which correspond to different ages within the early–middle Eocene time span, the reconstructed model shows these microfacies in a single section using Walter's Law. The palaeoenvironmental reconstruction (Fig. 10) is based on the 'distally-steepened ramp' model by Handford and Loucks (1993) and also takes into account the ramp subdivision terminology by Burchette and Wright (1992). The photic framework by Pomar (2001) and Pomar et al. (2017) is also considered and the 'mesophotic zone' is present in the model. The uppermost boundary of this mesophotic zone corresponds to the lower limit of the 'uppermost photic zone' of Hottinger (1997), at approximately 40 m depth, marking the deepest occurrence of marine vegetation (Pomar, 2001). The lowermost boundary coincides with the 'upper photic zone' of Hottinger (1997), at approximately 80 m depth and the disappearance of deeper hyaline larger benthic foraminifera (orthophragminids). The morphological terminology for the crustose coralline red algae is that used by Nebelsick and Bassi (2000).

#### 5.1.1. Inner ramp

This depositional environment is recognised from microfacies *Mf1* (quartz-rich calcarenites with larger benthic foraminifera packstone) and *Mf3* (porcelaneous larger benthic foraminifera and rotaliid-rich packstone–grainstone), found in the lower portion (Cuisian) of stratigraphic sections 1 (Oued el Lile) and 2 (Aghermame) (Fig. 10). *Mf1* (quartz-rich calcarenites with larger benthic foraminifera packstone) represents the intermediate portion of the inner ramp marked by a larger benthic foraminifera-rich biotic assemblage, including alveolines and a diverse association of hyaline larger benthic foraminifera (nummulites, assilines, discocyclus, amphistegines and rotaliids) in an echinoid

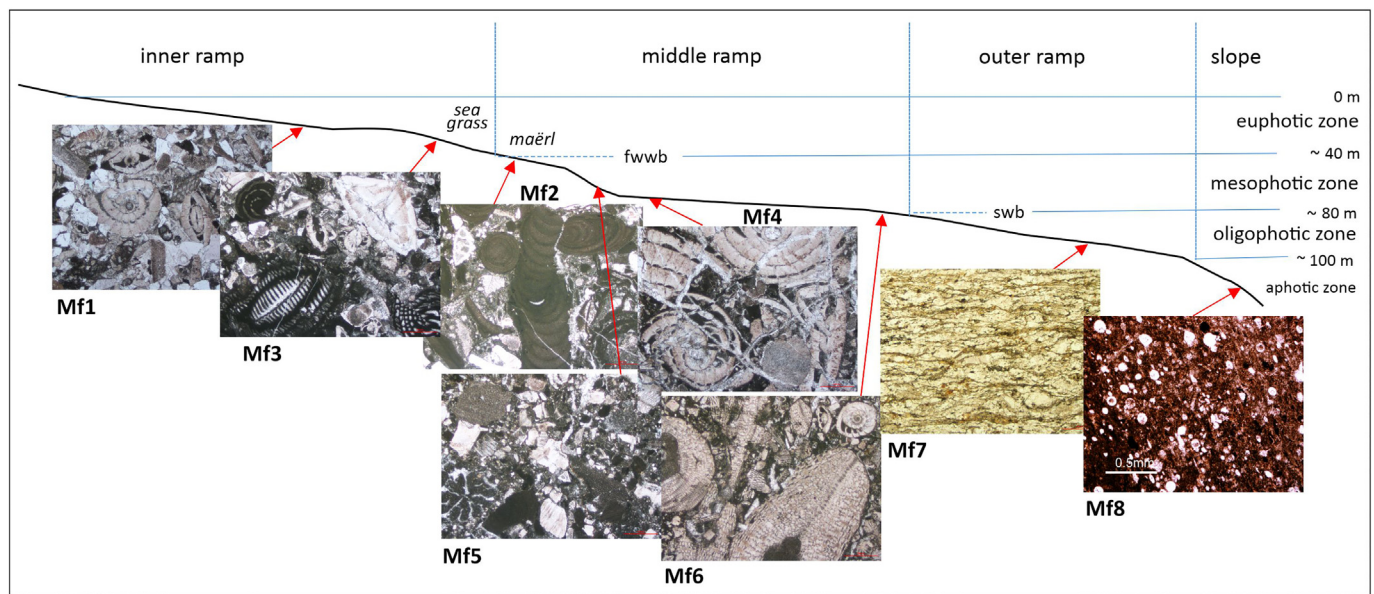


**Fig. 10.** The environmental microfacies distribution for the lower–middle Eocene marine Ghomaride succession. *Mf1*, 'transgressive reworked deposit' in the inner ramp, upper subtidal environment; *Mf2*, mid ramp maërl environment; *Mf3*, inner ramp sea-grass environment; *Mf4*, mid ramp hyaline larger benthic foraminifera accumulations (nummulitids); *Mf5*, distal mid ramp maërl environment; *Mf6*, distal mid ramp larger benthic foraminifera accumulations (orthophragminids); *Mf7*, outer ramp (circalittoral) environment; *Mf8*, slope environment. Legend: fwwb (fair weather wave base); swb (storm wave base).

debris-rich matrix. Alveolines are often found in oligotrophic shallow-marine habitats without sea-grass cover (Hottinger, 1983, 1997; Spanicek et al., 2017), whilst the dominance of hyaline larger benthic foraminifera is more characteristic of oligotrophic and mesophotic marine habitats in mid ramp settings (Hottinger, 1983, 1997). The echinoid-rich debris indicates mesotrophic conditions and the numerous rounded quartz grains suggest proximity to the continent. The other common components observed in *Mf1* (quartz-rich calcarenites with larger benthic foraminifera packstone) are part of a heterotrophic association consisting of bivalve molluscs, bryozoans, annelids, small benthic (textulariids, discorbids) and rare planktic foraminifera, which denote the mesotrophic character of the environment. This mixture of components could be interpreted as a reworked deposit during a transgressive phase with the influence of siliciclastic supply from adjacent emerged land areas in euphotic and subtropical marine conditions. *Mf3* (porcelaneous larger benthic foraminifera and rotaliid-rich packstone–grainstone), on the other hand, shows a notable presence of orbitolites, miliolids, dasyclade algae (*Ovulites?*), discorbids and textulariids, an assemblage characteristic of a sea-grass marine substrate (meadows: Langer, 1993; Hottinger, 1997; Beavington-Penney et al., 2004; Reich et al., 2015; Tomás et al., 2016; Martín-Martín et al., 2020c, 2021; Tosquella et al., 2022). This assemblage is included in an alveoline/rotaliid-rich sediment, typically occurring in inner ramp environments in non-vegetated substrates (Hottinger, 1997; Spanicek et al., 2017). This supports the idea of alveoline reworking, suggesting inner marine conditions that are different from those of *Mf1* (quartz-rich calcarenites with larger benthic foraminifera packstone), with clear evidence of the influence of marine waves and currents that supply a significant number of mid-ramp hyaline larger benthic foraminifera tests (such as nummulites, assilines, discocyclines and amphistegines), as well as rhodophycean and solenomerid remains, to the shallowest part of the ramp (Hottinger, 1983, 1997). Generally, a porcelaneous larger benthic foraminifera association characterises oligotrophic environments in the euphotic inner ramp setting, but the significant presence of mid-ramp hyaline larger benthic foraminifera tests and other biotic elements, such as planktic foraminifera, suggests a significant marine influence by waves and currents from the neighbouring open ramp to shallower environments. From a trophic perspective, the presence of frequent plate and spine remains of echinoids, ostracods, bryozoans and small benthic foraminifera of uncertain origin indicates local mesotrophic-to-eutrophic conditions due to seafloor reworking during storm periods.

### 5.1.2. Mid ramp

The mid ramp depositional environment is recognised from the microfacies *Mf2* (hyaline larger benthic foraminifera-rich coral–foralgal rudstone), *Mf4* (nummulite packstone), *Mf5* (hyaline larger benthic foraminifera-rich coral–foralgal boundstone) and *Mf6* (discocycline packstone), which are observed in the lower and middle portions (Cuisian–Lutetian) of the three studied stratigraphic sections (Fig. 10).

*Mf2* (hyaline larger benthic foraminifera-rich coral–foralgal rudstone) shows a greater marine influence than the previous microfacies and could represent a mid ramp maërl environment. Porcelaneous larger benthic foraminifera tests are not present in this facies, whilst rhodoliths, solenomerid macroids and hyaline larger benthic foraminifera tests are very abundant. The observation of rare z-coral cobbles suggests the presence of neighbouring reef growths, indicating warm water and high-light conditions in shallow-marine environments. The hyaline larger benthic foraminifera association, composed of abundant tests of discocyclines, nummulites, assilines, amphistegines and larger rotaliids, is characteristic of mesophotic mid ramp settings (Hottinger, 1983, 1997). Coralline crustose algae are present both as free-living lumped *Sporolithon* rhodoliths and sometimes as the coating on solenomerid macroids as the nucleus of growth. Furthermore, *Solenomeris* macroids are sometimes wrapped by other acervulinids, such as *Acervulina linearis*. All these assemblages and the presence of

reworked z-coral cobbles suggest a medium to coarse-grained mobile substrate in the innermost part of mid ramp environments. The remaining part of the biotic association observed in this facies is clearly heterotrophic and composed of echinoid debris, bryozoans, ostracods, textulariids and other small benthic and planktic foraminifera of uncertain origin. This suggests mesotrophic conditions, in contrast to the dominant oligotrophic larger benthic foraminifera and z-coral assemblage. All these features reinforce the idea that much of the biotic association that characterises this microfacies is reworked, possibly due to storm events in a transgressive context. Reworking provides bioclastic material from the mid ramp to inner marine environments and return marine currents, acting in the opposite direction, are indicated by the presence of z-coral cobbles from innermost marine settings. The poorly sorted *Mf5* (hyaline larger benthic foraminifera-rich coral–foralgal boundstone) with a boundstone texture can also be observed. This facies displays abundant rhodolite structures growing on z-coral and ostreid cobbles, as well as foralgal structures (rhodolites/macroids) composed of multilayered crustose coralline and hyaline foraminifer encrusters (solenomerids and other acervulinids) and a matrix rich in hyaline larger benthic foraminifera and abundant nummulites, discocyclines, amphistegines, assilines and operculiniform assilines. The presence of this mid-ramp larger benthic foraminifera assemblage, along with the significant amount of rhodolite and foralgal remains, possibly reworked from innermost environments, suggests distal mid ramp maërl settings. Microfacies *Mf4* (nummulite packstone) and *Mf6* (discocycline packstone), nummulite and discocycline packstone, respectively, do not show significant foralgal character (rhodoliths and/or macroids), which indicates open marine settings compared to the previous microfacies *Mf2* (hyaline larger benthic foraminifera-rich coral–foralgal rudstone) and *Mf5* (hyaline larger benthic foraminifera-rich coral–foralgal boundstone). *Mf4* (nummulite packstone) could occupy the mid portion of the mid ramp, whilst the discocycline packstone would be located in the outermost part. In both cases, the dominance of hyaline larger benthic foraminifera tests suggests oligotrophic conditions. However, the presence of other biotic elements, such as planktic foraminifera, rotaliids, textulariids, bolivinids, sphaerogypsines and other small benthic foraminifera, ostracods, bryozoans, echinoid spines and plates and mollusc remains indicates mesotrophic-to-eutrophic conditions during some sedimentary intervals, which could be related to upwelling currents in neighbouring oceanic areas.

### 5.1.3. Outer ramp-slope

This depositional environment is recognised from microfacies *Mf7* (azoic quartzsiltite) and *Mf8* (marly–siltitic wackestone with radiolarians), which are observed in the upper portion (Lutetian–Bartonian) of stratigraphic sections 1 (Oued el Lile) and 2 (Aghermene) (as shown in Fig. 10).

*Mf7* (azoic quartzsiltite) consists of monotonous, azoic quartzsiltite with a significant presence of rounded fine-sized quartz grains and is strongly foliated by tectonics. Planktonic foraminifera have been observed only in the levigates. This facies always covers the *Mf5* (hyaline larger benthic foraminifera-rich coral–foralgal boundstone) microfacies and represents the uppermost part of the Oued el Lile section. The upper part of the Aghermene section is covered by the radiolaritic facies *Mf8* (marly–siltitic wackestone with radiolarians). This stratigraphic position suggests open marine settings corresponding to an oligophotic outer ramp environment. *Mf8* (marly–siltitic wackestone with radiolarians) is a marly–siltitic sediment with a wackestone appearance and abundant spherical specimens of radiolarians, which suggest equatorial eutrophic upwelling settings in the uppermost part of the slope environment (Palmer, 1986; Bak et al., 1997; Lazarus, 2013; De Wever et al., 2014).

## 5.2. Palaeoenvironmental evolution

In the Ghomaride Domain, the Eocene sedimentary record is represented only by Cuisian to Bartonian deposits arranged in a general

deepening succession (Fig. 11). The succession, marked at its base by a regional unconformity, is divided into two depositional sequences separated by another unconformity and an associated stratigraphic gap spanning from late Cuisian to early Lutetian, probably related to a regional shallowing period with emersion and/or erosion (Martín-Martín et al., 2020c, 2021; Tosquella et al., 2022).

The lower depositional sequence (lower–middle Cuisian) consists of two minor deepening depositional cycles. The first transgressive cycle, from lower to middle Cuisian, is represented by a transgressive basal unit resting on the Jurassic substrate. This interval is composed of a larger benthic foraminifera-rich mixed assemblage of inner-to-mid ramp deposits with a notable presence of subrounded quartz grains. This interval seems to form part of a ‘transgressive lag deposit’ on the Jurassic basement and is composed of a larger benthic foraminifera-rich mixed assemblage of inner-to-mid ramp deposits with a notable presence of subrounded quartz grains. This composition suggests proximity to the continent and, therefore, the euphotic and mesotrophic (Hottinger, 1983) character of the depositional setting. This unit is followed by a coral–foralgal rudstone with numerous rhodolith structures in a limestone matrix with abundant hyaline larger benthic foraminifera, deposited in a maërl setting in the proximal part of the mid ramp, denoting mesophotic and mesotrophic ecological conditions.

The second transgressive cycle, middle Cuisian in age, starts with porcelaneous larger benthic foraminifera-rich limestone representing a sea-grass meadow setting in the inner ramp, followed by deposits rich in rhodolith and macroid structures (maërl) and finally by a discocycline-rich limestone interval. This cycle evolves from euphotic and mesotrophic conditions in the sea-grass to mesophotic habitats in the upper part of the sedimentary cycle, with a mesotrophic maërl unit deposited in the innermost part of the mid ramp, followed by an oligotrophic discocycline-rich interval from a distally mid ramp setting. This interval is capped by the aforementioned unconformity, representing a stratigraphic gap in the stratigraphic succession covering the late Cuisian–early Lutetian period. As mentioned above this unconformity belongs to a regional shallowing period with emersion and/or erosion without a main tectonic interference (Martín-Martín et al., 2020c, 2021; Tosquella et al., 2022).

The upper depositional sequence (middle Lutetian to Bartonian), lying above the described unconformity, is also characterised by a transgressive evolutionary trend. The sequence starts with a mainly oligotrophic nummulite-rich interval, which alternates and evolves into a mainly mesotrophic coral–foralgal boundstone included in a hyaline larger benthic foraminifera-rich matrix, deposited in a neighbouring area to the previous interval in the mesophotic innermost mid ramp environment. These

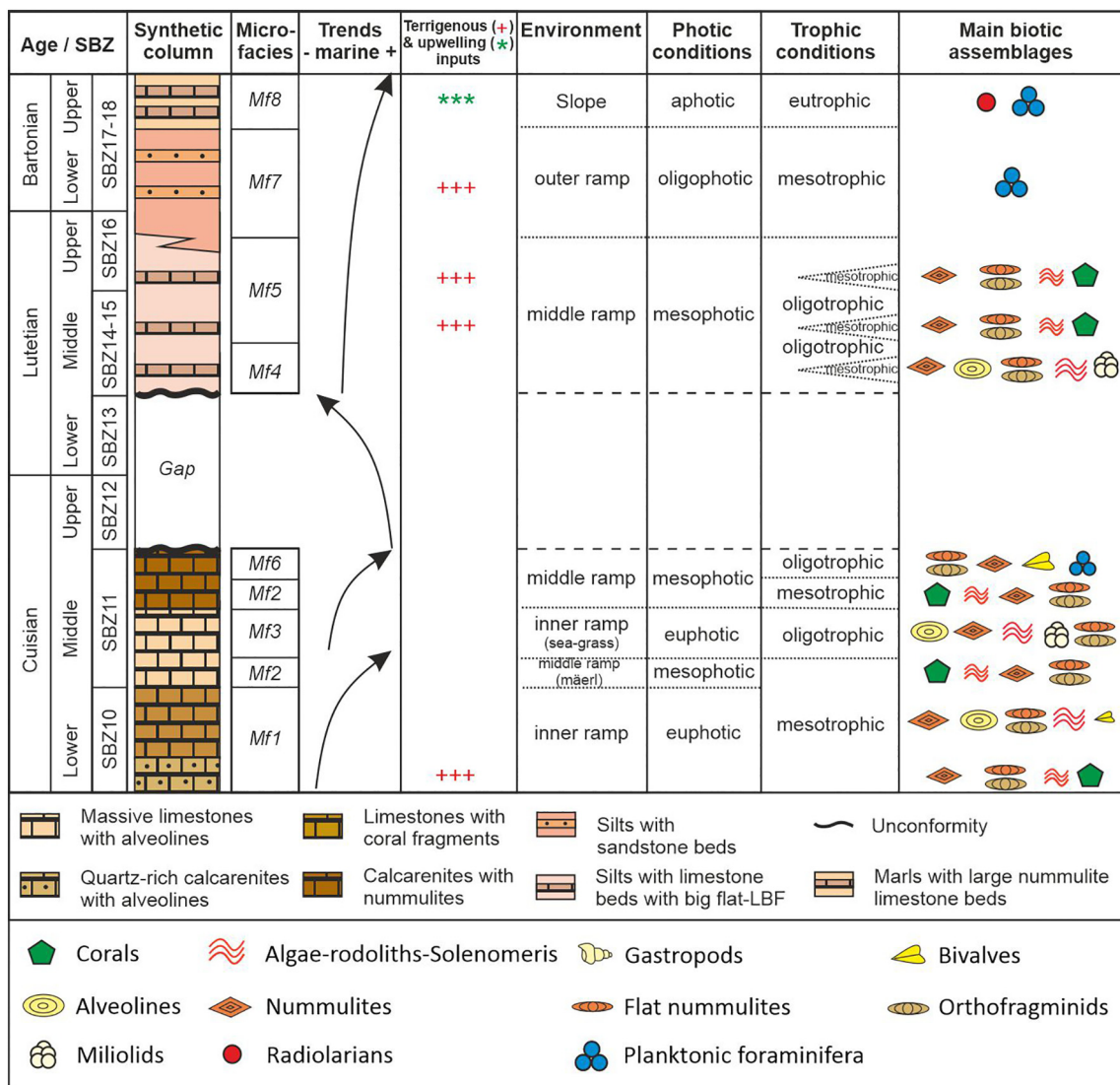


Fig. 11. A synthetic column of the Eocene Ghomaride succession, highlighting the correlation with transgressive–regressive depositional trends, terrigenous–nutrient inputs, sedimentary environments, photic and trophic conditions and main biotic assemblages.

deposits are covered in gradual transition by quartz–siltites with planktic foraminifers, representing an oligophotic and mesotrophic setting in the outer ramp. The succession ends with a marly–siltitic interval with abundant spheric radiolarians, possibly deposited in an aphotic and mesotrophic-to-eutrophic upper slope environment.

### 5.3. Ramp facies zones and carbonate factories

The Cuisian–Bartonian fossiliferous assemblage of the analysed stratigraphical sections shows a mixture of photozoan and heterotrophic elements. The photozoan association is composed of abundant larger benthic foraminifera, common crustose red algae, scarce colonial corals and rare dasyclad green algae, suggesting euphotic to mesophotic conditions in oligotrophic to mesotrophic marine warm waters at low–middle latitudes. The heterotrophic assemblage is composed of small benthic and planktic foraminifers, radiolarians, ostracods, molluscs, echinoids, bryozoans, annelids and other filter-feeding organisms. This assemblage may appear associated with photozoan components or isolated as a unique association and is always distributed in mobile mosaics (*sensu* Wright and Burgess, 2005), which are included in marine facies belts characterised by a fossil content in parallel with the environmental subdivision of the ramp. Their presence indicates a stationary supply of nutrients of continental origin or from upwelling currents in neighbouring areas, generating mesotrophic-to-eutrophic ecological conditions in the mainly oligotrophic depositional environment.

These marine belts are distributed from inner marine environments to open marine settings in the outer ramp and slope, each with a characteristic fossil assemblage. Inner ramp settings are characterised by oligotrophic sea-grass meadows and mesotrophic conditions, with a mixture of other larger benthic foraminifera from open marine environments in a transgressive sedimentary context. The inner part of the mesophotic mid ramp is represented by mesotrophic maërl environments that evolve distally into coral–foralgal boundstones. The rest of the mid ramp is oligotrophic and dominated by hyaline larger benthic foraminifera-rich belts, with nummulite-rich deposits in inner settings and discocycline-rich sediments in deeper settings. Oligophotic outer ramp environments are poorly differentiated, with only the presence of scattered planktic foraminifers in a mesotrophic matrix of quartz silt and their stratigraphic position, allowing identification of these environments. The quartz content is likely originated from temporary increases in nutrient availability due to river discharges and detrital supply or dusting provenance. Meso- to eutrophic aphotic slope environments are interpreted from the presence of spherical radiolarians as the only fossiliferous representation and from their position at the top of the transgressive trend of the upper depositional sequence. The presence of neighbouring upwelling environments is perfectly plausible in these circumstances. From a carbonate ‘factory’ perspective, the mixture of autotrophic (green and rhodophycean algae), mixotrophic (zooxanthellate corals and larger benthic foraminifera) and heterotrophic filter-feeding elements (bivalve molluscs, echinoid remains, bryozoans, small benthic and planktic foraminifers, ostracods and radiolarians), representing a wide range of trophic and light conditions of the sedimentary environment, allows us to propose a model analogous to the warm-temperate province (Betzler et al., 1997), the heterozoan (James, 1997), the transitional heterozoan–photozoan carbonate system (Halfar et al., 2004), or the heterozoan warm-water carbonates (Westphal et al., 2010). Generally, we consider the photozoan assemblage related to mainly oligotrophic warm-water conditions in low-latitude settings (tropical) (Hottinger, 1983; Hallock, 1988; Hottinger, 1997). However, the presence of phases of nutrient-enrichment, related or not to a decrease in marine water temperature, involves the development of a mainly filter-feeding biological assemblage (heterozoan), more typical of non-tropical environments, which makes it difficult to analyse and can lead to misinterpretation of climatic conditions (James, 1997; Halfar et al., 2004; Westphal et al., 2010). In the sedimentary profile of the carbonate factory, we include our

model (Fig. 10) in a transitional position between the “warm-temperate, transport-dominated accumulation” and the “warm-temperate, oligotrophic, distally-steepened ramp” (*sensu* Michel et al., 2018). All these data allow us to approach the palaeogeographic and palaeoceanographic settings of the studied area.

### 5.4. Trophic resources, larger benthic foraminifera-coral, and climatic events in the Tethyan area

The first appearance of larger benthic foraminifera in the Ghomaride Domain occurs in Cuisian deposits (Fig. 11). However, the first appearance of main generic taxa analysed in this work (nummulites) occurs at a global scale at the base of the lower Eocene (Ilerdian), but sedimentation of this stage is not represented in the area (Fig. 12). Climatic and/or tectonic causes can be the one responsible for the Eocene deepening, that took place at the base of Ilerdian in most Tethyan domains, but occurred later (Cuisian) in the Ghomaride sector.

From the analysis of fossil assemblages of Cuisian sediments in the studied area, the inner to mid ramp mesotrophic conditions developed during the lower Cuisian change clearly during the middle Cuisian evolving to mid ramp oligotrophic settings. Three coral events have been detected in the area during the Cuisian always appearing as reworked remains both in inner and mid ramp settings. The first coral event, at the lowermost part of Cuisian deposits (Shallow Benthic Zone 10), is found in a mesotrophic setting corresponding to a transgressive lag deposit influenced by terrestrial inputs. The second and third events have been found in the oligotrophic settings of the middle Cuisian deposits (Shallow Benthic Zone 11) in which larger benthic foraminifera (porcelaneous and hyaline), coralline algae and solenomerids were prevalent. Trophic data during the Cuisian differs in this area from the main highly oligotrophic global conditions proposed by Hallock et al. (1991), possibly associated to the coastal setting and the influence of continental waters. Only the oldest coral event could be correlated with the coral events recognised throughout the Tethyan region (Pomar et al., 2017; Martín-Martín et al., 2021). An important finding is the gap associated to a shallowing and emersion during late Cuisian–early Lutetian (Fig. 12) coinciding with the transition between the Early Eocene Climatic Optimum (EECO) and the start of the post-EECO Cooling throughout the Tethyan region (Zachos et al., 2001, 2008).

During the middle and late Lutetian, mainly oligotrophic conditions in mid ramp settings were developed in which mainly hyaline larger benthic foraminifera assemblages are prevalent, but the presence of two coral-rich interbedded levels denoting short-lived mesotrophic intervals (Shallow Benthic Zones 15–16) is remarkable. Both coral-events can be correlated with other Tethyan events (Fig. 12) at this time in the Pyrenean area (Pomar et al., 2017; Martín-Martín et al., 2021). These data partly differ from those of Hallock et al. (1991), which consider oligotrophic global conditions for the middle Lutetian and highly oligotrophic for the upper Lutetian. This period coincides with the Late Lutetian Thermal Maximum (LLTM) throughout the Tethyan region (Westerhold et al., 2018).

Finally, in the lower Bartonian deposits of the Ghomaride Domain take place the last occurrence of hyaline larger benthic foraminifera (Shallow Benthic Zone 17) and from this moment mainly mesotrophic and eutrophic conditions of sedimentation were developed in outer ramp and upper slope environments, as indicated by the presence of planktonic foraminifera and radiolarian-rich facies. This time interval coincides according to Hallock et al. (1991) with a global trophic transition from highly oligotrophic conditions to meso- and eutrophic settings at the end of the middle Eocene (Fig. 12). During this period there is no registered coral event in the study area in good agreement with the Tethyan record, whose recovery does not occur until the upper Bartonian (Pomar et al., 2017; Martín-Martín et al., 2021). This period coincides with the transition between the Mid Eocene Climatic Optimum (MECO) and the Mid–Late Eocene Cooling throughout the Tethyan region (Bohaty and Zachos, 2003; Zachos et al., 2008).

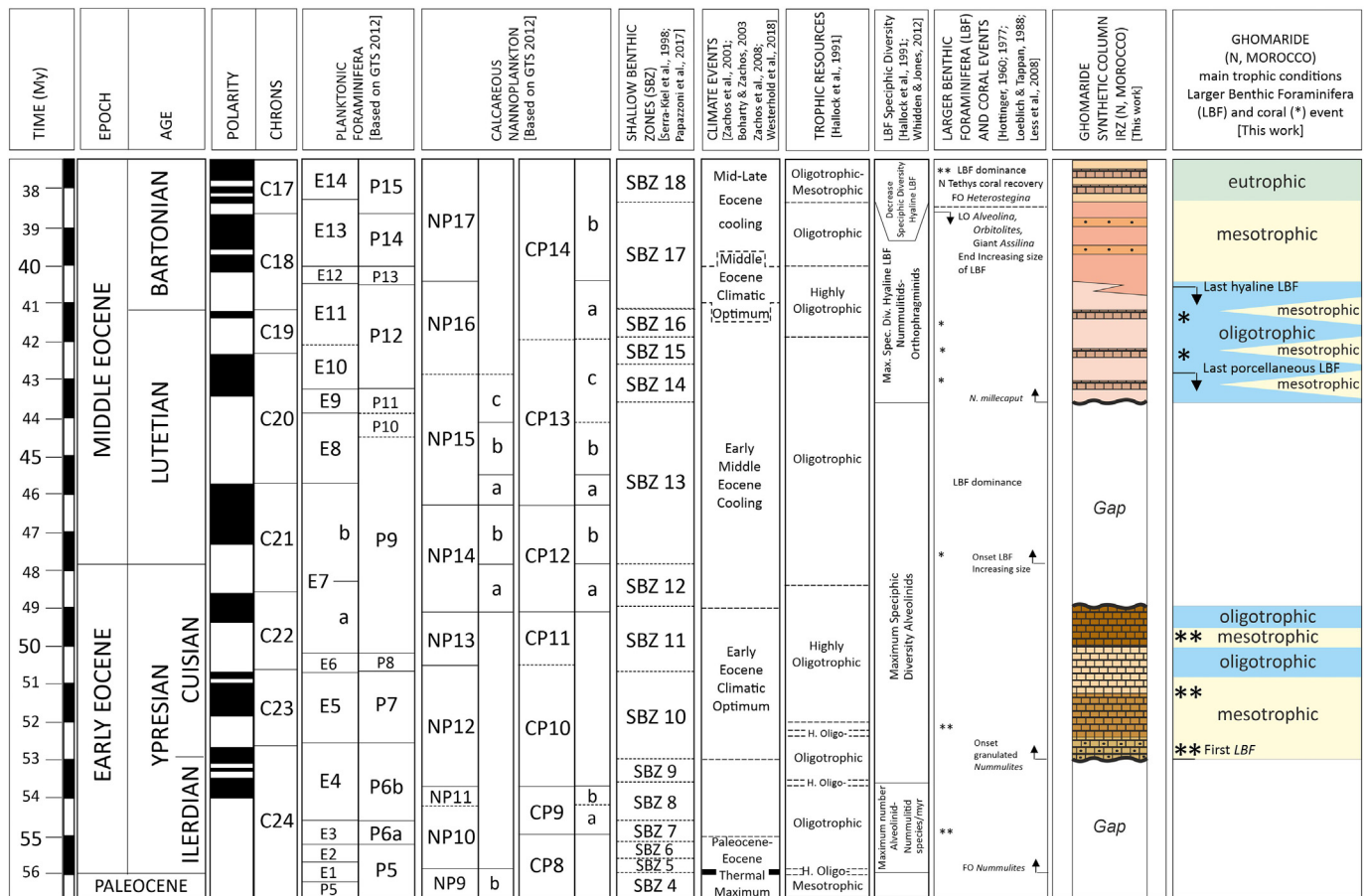


**Fig. 12.** A biostratigraphic chart that includes the numerical time scale, magnetochrons, magnetic polarity, planktonic foraminifera and calcareous nannoplankton zones based on GTS 2012 (Gradstein and Ogg, 2012). The figure also shows the correlations with Shallow Benthic Zones (Shallow Benthic Zone) and provides interpretations of the main climatic events, trophic resources continuum, larger benthic foraminifera specific diversity and coral events in the Tethyan Domain. A synthetic column is also included, which displays the stratigraphic formations, main trophic conditions, larger benthic foraminifera and coral (\*) events of the Eocene Ghomaride succession.

In general, when comparing the trophic conditions during the Cuisian–Bartonian time interval of the Ghomaride Domain with respect to the global trends proposed by Hallock et al. (1991), an increase in the degree of trophism (nutrients), is observed. This is probably in correspondence with the greater influence of continental inputs during the first part of this time interval, and potential upwelling at the end of this period.

5.5. Synthetic comparison with other sectors of the Tethyan Domain

The spatial and temporal distribution of Eocene platforms, depositional environments represented, the age and geometry of unconformities and the balance between larger benthic foraminifera and zooxanthellate corals are used to compare different Tethyan sectors (Fig. 13). The details of this comparison are supplied as Supplementary material A1 being presented here only a synthesis of the main findings. The northern Tethyan belt (S-Iberian margin, Pyrenean, Adriatic, Carpathian and Anatolian domains) is characterised by shallow-marine platform deposits from the Ilerdian to Bartonian, usually divided by sequence boundaries at the Ilerdian–Cuisian and Cuisian–Lutetian boundaries. The Pyrenean Domain has the most complete and deeply studied succession. Shallow-marine platforms usually consist of larger benthic foraminifera-rich deposits from inner-to-mid ramp environments with occasional z-coral build-ups except for the S-Iberian margin (Prebetics).

The southern Tethyan belt (Moroccan Atlas, Algeria, Tunisia, Libya, Egypt, Iran, Arabia, Oman, Yemen and Iran domains) is characterised by shallow-marine platform deposits from the upper Ypresian (Cuisian)

to Bartonian. The difference in deposition is believed to be related to the delay of tectonic deformation in the northern belt (affected by the Eo-Alpine tectonic phase during the Eocene) compared to the southern belt (barely affected by the Eo-Alpine phase) (Guerrera et al., 2021). The entire succession is typically divided by a sequence boundary at roughly the Cuisian–Lutetian boundary. Shallow-marine platforms are generally characterised by inner-to-mid ramp deposits, but a clear west–east difference is observed. In the west (Morocco to Tunisia), Eocene marine platforms are characterised by the absence or trace of larger benthic foraminifera and corals, favouring the expansion of oyster reefs and other heterotrophic elements. In the eastern part (Libya, Egypt, Arabia, Oman, Yemen and Iran), corallgal reefs and larger benthic foraminifera-rich facies developed.

The intermediate belt, located in microplates in the central-western Tethyan area, is similar to the Ghomaride Domain. This is the case of the Malaguide Domain in Southern Spain, where two types of successions have been recently described. In the central-western sector (Almería and Málaga), the Malaguide succession is discontinuous and reduced, with affinities to the Ghomaride succession (Cuisian to middle Lutetian; Tosquella et al., 2022), affected by a stratigraphic unconformity (early Lutetian). In the Malaguides from Almería and Málaga (Southern Spain), larger benthic foraminifera rich inner-mid ramp deposits with local intervals characterised by a relative presence of zooxanthellate corals are observed. In contrast, the Malaguide record of the eastern Betic sector (Sierra Espuña) is more complete, where the Cuisian to lower Lutetian deposits are recorded, with small z-coral build-ups in the lower Cuisian. Here, the middle to upper Eocene sedimentary record evolves to the outer ramp and slope environments. The higher presence

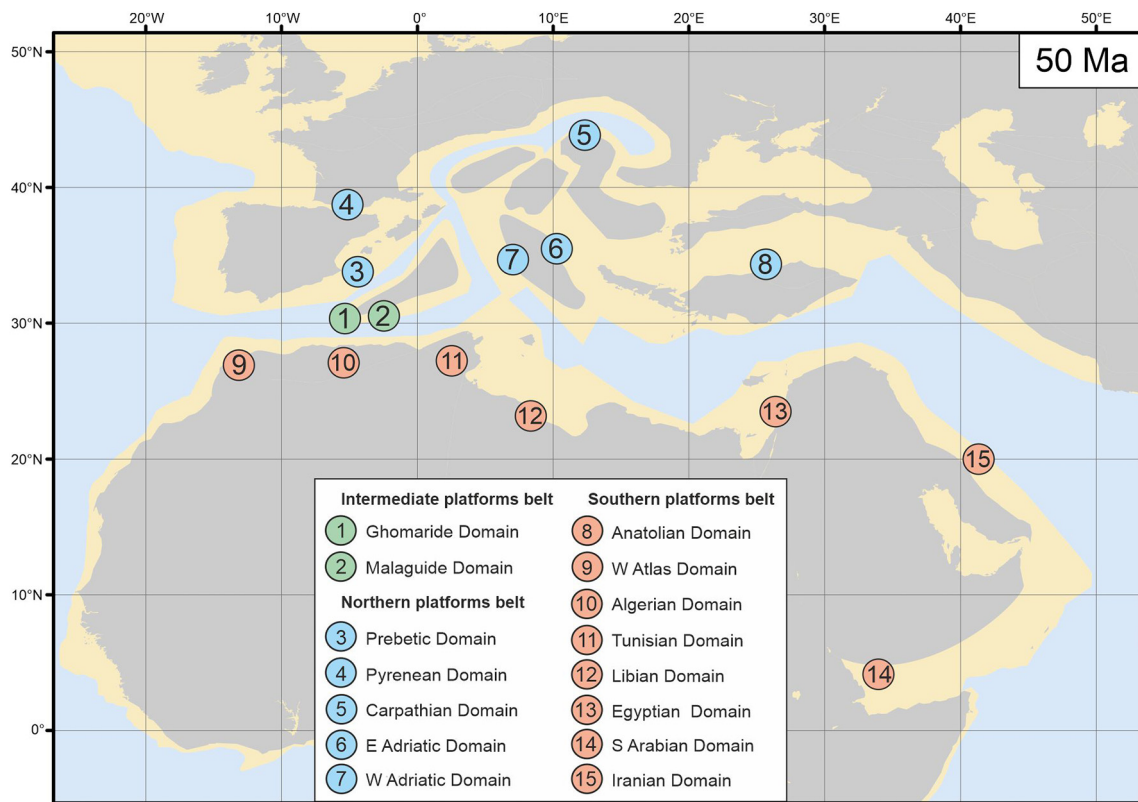


**Fig. 13.** Palaeogeographic sketch map near the Cretaceous/Cenozoic boundary (70 Ma) based on Gplates maps, which shows the location of the study area and the Tethyan sectors being compared.

(After Scheibner and Speijer (2008); Müller et al. (2019); Van Hinsbergen et al. (2020); Martín-Martín et al. (2020b, 2022); Le Breton et al. (2021).)

of zooxanthellate corals in some periods suggests a colder surface marine water environment compared to the Ghomaride area (Martín-Martín et al., 2020c; Coletti et al., 2022).

The widespread distribution of larger benthic foraminifera during the Eocene caused the decline or significant reduction of coral constructions (Scheibner and Speijer, 2008; Pomar et al., 2017; Martín-Martín et al., 2020c; Tosquella et al., 2022). However, a wide presence of z-corals was observed in several areas of the Tethys, demonstrating that coral growth persisted in this domain. The transition in global temperature conditions during the Ypresian–Lutetian period led to the local survival of corals in certain areas that should favour larger benthic foraminifera than corals, which could be associated with short-lived events of a slight decrease in mean sea-water surface temperatures (Hallock, 2000; Scheibner and Speijer, 2008; Pomar et al., 2017; Martín-Martín et al., 2021).

The atypical situation mentioned in the western part of the southern belt, where oysters and other heterotrophic elements dominated the Eocene platforms instead of larger benthic foraminifera–coral associations, can be attributed to the presence of nutrient-rich upwelling currents in the Moroccan Atlas Domain. These conditions should be unfavourable for the growth of larger benthic foraminifera and corals, since they rely on photosynthesis by their internal algal symbionts rather than the environmental supply of nutrients (Föllmi, 1996; Martín-Martín et al., 1998).

The Ghomaride Domain is an intermediate case between the northern platform belt and the eastern part of the southern belt, where larger benthic foraminifera dominate over zooxanthellate corals, even though the latter are not entirely absent or as well developed as in other domains.

According to the data presented above (Fig. 12) for the Eocene studied period, during warm intervals as the Early Eocene Climatic Optimum (EECO; Zachos et al., 2001), Late Lutetian Thermal Maximum (LLTM; Westerhold et al., 2018) and Middle Eocene Climatic Optimum (MECO; Bohaty and Zachos, 2003; Zachos et al., 2008), carbonate platform deposits took place in the Ghomaride Domain. Nevertheless, a

delay in the Early Eocene carbonate platform is registered in this domain with respect to other Tethyan domains. In the case of the Ghomaride this deepening took place in the Cuisian, whilst in other Tethyan areas it took place earlier, in the Ilerdian. Also, during the most of Bartonian times (mid–late Eocene cooling) a deepening in marine sedimentation is registered in the Ghomaride area until the end of the Eocene, whilst other Tethyan domains show shallowing and emersion. Both anomalies detected in the Ghomarides can be attributed to particular climatic conditions or local tectonic interferences.

## 6. Conclusions

1. The study of three stratigraphic sections allowed reconstructing the Eocene carbonate platforms on the Ghomarides Complex (Internal Rif Zones), located in the westernmost Tethys at approximately 30°N and 0°–10°W.
2. The Eocene sedimentary record (Cuisian to Bartonian) is arranged in a general transgressive trend. The succession, marked at its base by a regional unconformity, is divided into two depositional sequences separated by another unconformity and an associated stratigraphic gap spanning from late Cuisian to early Lutetian (Shallow Benthic Zones 12–13). The lower depositional sequence is Cuisian *p.p.* (Shallow Benthic Zones 10–11) and consists in two minor transgressive depositional cycles, whilst the upper sequence is middle Lutetian *p.p.* to Bartonian (Shallow Benthic Zones 14–17).
3. The fossiliferous assemblage, texture and fabric analysis have allowed the identification of eight microfacies (*Mf1* to *Mf8*) characterising the depositional environments in a ‘distally-steepened carbonate ramp’. The inner ramp was recognised from microfacies *Mf1* and *Mf3* (Cuisian). The mid ramp was recognised from microfacies *Mf2* and *Mf4–Mf6* (Cuisian and middle Lutetian). The outer ramp-slope was recognised from microfacies *Mf7* and *Mf8* (upper Lutetian–Bartonian).

4. The fossiliferous assemblages analysed show a mixture of photozoan and heterotrophic elements. The photozoan association, composed by larger benthic foraminifera, crustose red algae, colonial corals and dasyclad green algae, characterises euphotic to mesophotic habitats in oligotrophic to mesotrophic marine warm waters at low–middle latitudes. The heterotrophic association, composed by small benthic and planktic foraminifera, radiolarians, ostracods, molluscs, echinoids, bryozoans, annelids and other filter-feeding organisms, appearing both mixing in previous association and in isolate levels, suggests short-lived events of nutrient input or general mesotrophic to eutrophic conditions.
5. In detail, the lower sedimentary cycle (lower Cuisian *p.p.*) represents euphotic to mesophotic inner to middle ramp environments (maërl) and mesotrophic conditions. The second cycle (middle Cuisian) shows euphotic to mesophotic inner (sea-grass) to mid ramp environments in mesotrophic to oligotrophic conditions. In contrast, the upper cycle (middle–upper Lutetian to Bartonian) was more extensive and dynamic. It represents mid ramp to slope environments, ranging from mesophotic–oligotrophic to aphotic conditions, in oligotrophic to mesotrophic and eutrophic settings.
6. The spatial and temporal distribution of Eocene platforms, represented by depositional environments, age and geometry of unconformities, and the balance between larger benthic foraminifera and zooxanthellate corals has been used to compare different Tethyan sectors. In general, when comparing the trophic conditions during the Cuisian–Bartonian time interval of the Ghomaride Domain with respect to the global trends, an increase in the degree of trophism (nutrients) is observed. This is probably in correspondence with the greater influence of continental inputs during the first part of this time interval, and potential upwelling at the end of this period.
7. The widespread global distribution of larger benthic foraminifera in the Eocene led to the disappearance or drastic reduction of coral constructions. However, the performed comparison in the western Tethys revealed the presence of abundant zooxanthellate corals in several areas. This suggests that corals could continue to develop under certain conditions even though larger benthic foraminifera should be better suited to them than corals. This can be interpreted as a product of short-lived events of a slight decrease in average temperature of sea surface waters. Furthermore, in some areas close to the Atlantic Ocean in the westernmost Tethys, oyster reefs replaced larger benthic foraminifera and coral associations in the Eocene platforms due to nutrient-rich upwelling currents that were unfavourable for photosynthetic organisms.
8. The Ghomaride platform domain, along with the Malaguide one, represents an intermediate case compared to the northern Tethyan platform belt and the eastern sector of the southern Tethyan belt. In these areas, larger benthic foraminifera are dominant over zooxanthellate corals, but they are never completely absent.
9. In the study area, during Eocene warm intervals a carbonate platform took place, whilst during the cooling ones shallowing and gaps in the sedimentation are registered. Two anomalies have been detected in the Ypresian and Bartonian times indicating particular climatic conditions or local tectonic interferences, deserving to be studied in depth in the future.

#### Data availability

Data will be made available on request.

#### Declaration of competing interest

The authors declare that they have no known competing financial interests or personal relationships that could have appeared to influence the work reported in this paper.

#### Acknowledgements

Research supported by: Research Project PID2020-114381GB-I00, Spanish Ministry of Science and Innovation; Research Groups and Projects from M. Martín-Martín, Alicante University (CTMA-IGA). We also thank reviewers for the very useful revision furnished.

#### Appendix A. Supplementary data

Supplementary data to this article can be found online at <https://doi.org/10.1016/j.sedgeo.2023.106423>.

#### References

- Adams, C.G., Lee, D.E., Rosen, B.R., 1990. Conflicting isotopic and biotic evidence for tropical seasurface temperatures during the Tertiary. *Palaeogeography, Palaeoecology, Palaeoclimatology* 77, 289–313.
- Bak, K., Bak, M., Geroch, S., Manecki, M., 1997. Biostratigraphy and paleoenvironmental analysis of benthic Foraminifera and radiolarians in Paleogene variegated shales in the Skole Unit, Polish Flysch Carpathians. *Annales. Societatis Geologorum Poloniae* 67 (2–3), 135–154.
- Beavington-Penney, S.J., Wright, V.P., Woelkerling, W.J., 2004. Recognising macrophyte-vegetated environments in the rock record: a new criterion using 'hooked' forms of crustose coralline red algae. *Sedimentary Geology* 166, 1–9.
- Betzler, C., Brachert, T.C., Nebelsick, J., 1997. The warm temperate carbonate province. A review of the facies, zonations, and delimitations. *Courier Forschungs-Institute Senckenberg* 201, 83–99.
- Bohaty, S.M., Zachos, J.C., 2003. Significant Southern Ocean warming event in the late middle Eocene. *Geology* 31 (11), 1017–1020.
- Bohaty, S.M., Zachos, J.C., Florindo, F., Delaney, M.L., 2009. Coupled greenhouse warming and deep-sea acidification in the middle Eocene. *Paleoceanography* 24, PA2207.
- Burchette, T.P., Wright, V.P., 1992. Carbonate ramp depositional systems. *Sedimentary Geology* 79, 3–57.
- Chalouan, A., 1986. Les nappes Ghomarides (Rif septentrional, Maroc), un terrain varisque dans la Chaîne Alpine. Univ. Louis Pasteur de Strasbourg (Tesis Doctoral, 371 pp.).
- Chalouan, A., Michard, A., 2004. The Alpine rift belt (Morocco): a case of mountain building in a subduction-subduction-transform fault triple junction. *Pure and Applied Geophysics* 161, 489–519.
- Chalouan, A., Michard, A., El Kadiri, K.H., Frizon de Lamotte, D., Soto, J.I., Saddiqi, O., 2008. Continental evolution: the geology of Morocco. *Lecture Notes in Earth Sciences* 116, 203–302 (Springer-Verlag Berlin Heidelberg).
- Coletti, G., Commissario, L., Mariani, L., Bosio, G., Desbiolles, F., Soldi, M., Bialik, O.M., 2022. Palaeocene to Miocene southern Tethyan carbonate factories: a meta-analysis of the successions of South-western and Western Central Asia. *The Depositional Record* 8, 1031–1054. <https://doi.org/10.1002/dep2.204>.
- De Wever, P., O'Dogherty, L., Gorican, S., 2014. Monsoon as a cause of radiolarite in the Tethyan realm. *Comptes Rendus Geoscience* 346 (11–12), 287–297.
- Dickens, G.R., Castillo, M.M., Walker, J.C.G., 1977. A blast of gas in the latest Paleocene: simulating first-order effects of massive dissociation of oceanic methane hydrate. *Geology* 25 (3), 259–262.
- Doglioni, C., 1992. Main differences between thrust belts. *Terra Nova* 4, 152–164.
- Embry, A.F., Klovan, J.E., 1971. A Late Devonian reef tract on Northeastern Banks Island, NWT. *Canadian Petroleum Geology Bulletin* 19, 730–781.
- Flügel, E., 2010. *Microfacies of Carbonate Rocks. Analysis, Interpretation and Application*. Springer (976 pp.).
- Föllmi, K.B., 1996. The phosphorous cycle, phosphogenesis and marine phosphate-rich deposits. *Earth-Science Reviews* 40, 55–124.
- Frizon de Lamotte, D., Zaghloul, M.N., Faouziya, H., Mohn, G., Leprêtre, R., Gimeno-Vives, O., Atouabat, A., El Mourabet, M., Abass, A., 2017. Rif externe: comment comprendre et expliquer le chaos apparent? *Géologues* 194, 13–15.
- Gradstein, F.M., Ogg, J.G., 2012. Chapter 2 - the chronostratigraphic scale. In: Gradstein, F.M., Ogg, J.G., Schmitz, M.D., Ogg, G.M. (Eds.), *The Geologic Time Scale*. Elsevier, pp. 31–42.
- Guerrera, F., Martín-Martín, M., Tramontana, M., 2021. Evolutionary geological models of the central-western peri-Mediterranean chains: a review. *International Geology Review* 63, 65–86.
- Halfar, J., Godínez-Orta, L., Mutti, M., Valdez-Holguín, J.E., Borges, J.M., 2004. Nutrient and temperature controls on modern carbonate production: an example from the Gulf of California, Mexico. *Geology* 32, 213–216.
- Hallock, P., 1988. Diversification in algal symbiont-bearing foraminifera: a response to oligotrophy. *Revue de Paléobiologie vol. spéc. 2 (Benthos'86)*, 789–797.
- Hallock, P., 2000. Symbiont-bearing foraminifera: harbingers of global change? *Micropaleontology* 46 (1), 95–104.
- Hallock, P., Premoli-Silva, I., Boersma, A., 1991. Similarities between planktonic and larger foraminiferal evolutionary trends through Paleogene paleoceanographic changes. *Palaeogeography, Palaeoecology, Palaeoclimatology* 83, 49–64.
- Handford, C.R., Loucks, R.G., 1993. Carbonate depositional sequences and systems tracts - responses of carbonate platforms to relative sea-level changes. In: Loucks, B., Sarg, R.J. (Eds.), *Carbonate Sequence Stratigraphy: Recent Developments and Applications*. AAPG Bulletinvol. 57, pp. 3–41.
- Herbig, H.G., Trappe, J., 1994. Stratigraphy of the Subatlas Group (Maastrichtian–Middle Eocene, Morocco). *Newsletters on Stratigraphy* 30, 125–165.

- Hlila, R., Maaté, A., Sanz de Galdeano, C., Serra-Kiel, J., Serrano, F., El Kadiri, Kh., 2007. La serie paleógena de la unidad superior del Gomáride en Talembote (Rif Interno, Marruecos). *Geogaceta* 43, 91–94.
- Höntzsch, S., Scheibner, C., Brock, J.P., Kuss, J., 2013. Circum-Tethyan carbonate platform evolution during the Palaeogene: the Prebetic platform as a test for climatically controlled facies shifts. *Turkish Journal of Earth Sciences* 22, 891–918.
- Hottinger, L., 1983. Processes determining the distribution of larger foraminifera in space and time. *Utrecht Micropaleontological Bulletin* 30, 239–253.
- Hottinger, L., 1997. Shallow benthic foraminiferal assemblages as signals for depth of their deposition and their limitations. *Bulletin de la Société Géologique de France* 168, 491–505.
- Jabaloy-Sánchez, A., Martín-Algarra, A., Padrón-Navarta, J.A., Martín-Martín, M., Gómez-Pugnaire, M.T., Sánchez-Vizcaíno, V.L., Garrido, C.J., 2019. Lithological successions of the internal zones and flysch trough units of the betic chain. In: Quesada, C., Oliveira, J.T. (Eds.), *The Geology of Iberia: A Geodynamic Approach*. Regional Geology Reviews. Springer Nature, pp. 377–432.
- James, N.P., 1997. The cool-water carbonate depositional realm. In: James, N.P., Clarke, J.A. D. (Eds.), *Cool-water Carbonates*. SEPM Spec. Publ. 56, pp. 1–22.
- Kennett, J.P., Stott, L.D., 1991. Abrupt deep-sea warming, palaeoceanographic changes and benthic extinctions at the end of the Palaeocene. *Nature* 353 (6341), 225–229.
- Koch, P.L., Zachos, J.C., Gingerich, P., 1992. Correlation between isotope records in marine and continental carbon reservoirs near the Palaeocene/Eocene boundary. *Nature* 358, 319–322.
- Langer, M.R., 1993. Epiphytic foraminifera. *Marine Micropaleontology* 20, 235–265.
- Langer, M.R., Hottinger, L., 2000. Biogeography of selected larger foraminifera. *Micropaleontology* 46 (Suppl. 1), 105–126.
- Lazarus, D., 2013. Palaeoceanography, biological proxies: radiolarians and Silicoflagellates. In: Elias, S.A., Mock, C.J. (Eds.), *Encyclopedia of Quaternary Science*, 2nd ed. Elsevier, pp. 830–840.
- Le Breton, E., Brune, S., Ustaszewski, K., Zahirovic, S., Seton, M., Müller, R.D., 2021. Kinematics and extent of the Piemont-Liguria Basin-implications for subduction processes in the Alps. *Solid Earth* 12, 885–913.
- Leprêtre, R., Frizon de Lamotte, D., Combie, R.V., Gimeno-Vives, O., Mohn, G., Eschard, R., 2018. The Tell-Rif orogenic system (Morocco, Algeria, Tunisia) and the structural heritage of the southern Tethys margin. *Bulletin Société Géologique France: Earth Sciences Bulletin* 189, 10. <https://doi.org/10.1051/bsgf/2018009>.
- Loeblich, A.R., Tappan, H.P., 1988. Foraminiferal Genera and Their Classification. vol. 2. Van Nostrand Reinhold Company (970 pp.).
- Maaté, A., 1984. Etude géologique de la couverture mésozoïque et cénozoïque des unités Ghomarides au Nord de Tétouan (Rif interne, Maroc). Université de Toulouse (Tesis doctoral, 161 pp.).
- Maaté, A., 1996. Estratigrafía y Evolución paleogeográfica alpina del Dominio Gomáride (Rif Interno, Marruecos). Universidad de Granada (Tesis Doctoral, 397 pp.).
- Maaté, A., Martín-Algarra, A., Martín-Martín, M., Serra-Kiel, J., 2000. Nouvelles données sur le Paléocène-Eocène des zones internes bético-rifaines. *Geobios* 33, 409–418.
- Martín-Algarra, A., 1987. Evolución geológica Alpina del contacto entre las Zonas Internas y las Zonas Externas de la Cordillera Bética. Universidad Granada (Unpublished PhD Thesis, 1171 pp.).
- Martín-Martín, M., Serra-Kiel, J., El Manoune, B., Martín-Algarra, A., Serrano, F., 1998. The Paleocene of the Eastern Malaguides (Betic Cordillera, Spain): stratigraphy and paleogeography. *Comptes Rendus Geoscience* 326, 35–45.
- Martín-Martín, M., Guerrero, F., Tramontana, M., 2020a. Geodynamic implications of the latest Chattian-Langhian central-western peri-Mediterranean volcano-sedimentary event: a review. *The Journal of Geology* 128. <https://doi.org/10.1086/706262>.
- Martín-Martín, M., Guerrero, F., Miçlaus, C., Tramontana, M., 2020b. Similar Oligo-Miocene tectono-sedimentary evolution of the Paratethyan branches represented by the Moldavian Basin and Maghreb Flysch Basin. *Sedimentary Geology* 396, 105548.
- Martín-Martín, M., Guerrero, F., Tosquella, J., Tramontana, M., 2020c. Paleocene–Lower Eocene carbonate platforms of westernmost Tethys. *Sedimentary Geology* 404, 105674.
- Martín-Martín, M., Guerrero, F., Tosquella, J., Tramontana, M., 2021. Middle Eocene carbonate platforms of the westernmost Tethys. *Sedimentary Geology* 415, 105861.
- Martín-Martín, M., Guerrero, F., Maaté, A., Hlila, R., Serrano, F., Cañaveras, J.C., Paton, D., Alcalá, F.J., Maaté, S., Tramontana, M., Martín-Pérez, J.A., 2022. The Cenozoic evolution of the Intra-Rif (Rif, Morocco). *Geosphere* 18 (2), 850–884.
- Michard, A., Chalouan, H.A., Feinbergh, H., Goffe, B., Montigny, R., 2002. How does the Alpine belt end between Spain and Morocco? *Bulletin de la Société Géologique de France* 173, 3–15.
- Michard, A., Frizon de Lamotte, D., Liégeois, J.-P., Saddiqi, O., Chalouan, A., 2008. Conclusion: continental evolution in Western Maghreb. In: Michard, A., Saddiqi, O., Chalouan, A., Frizon de Lamotte, D. (Eds.), *Lecture Notes in Earth Sciences* vol. 116 (404 pp.).
- Michard, A., Saddiqi, O., Missenard, Y., Oukassou, M., Barbarand, J., 2017. Les grandes régions géologiques du Maroc; diversité et soulèvement d'ensemble. *Géologues* 194, 1–11.
- Michel, J., Borgomano, J., Reijmer, J.G., 2018. Heterozoan carbonates: when, where and why? A synthesis on parameters controlling carbonate production and occurrences. *Earth-Science Reviews* 182, 50–67.
- Müller, R.D., Zahirovic, S., Williams, S.E., Cannon, J., Seton, M., Bower, D.J., Tetley, M.G., Heine, C., Le Breton, E., Liu, S., Russell, S.H.J., Yang, T., Leonard, J., Gurnis, M., 2019. A global plate model including lithospheric deformation along major rifts and orogens since the Triassic. *Tectonics* 38. <https://doi.org/10.1029/2018TC005462>.
- Nebelsick, J.H., Bassi, D., 2000. Diversity, growth forms and taphonomy: key factors controlling the fabric of coralline algae dominated shelf carbonates. In: Insalaco, E., Skelton, P.W., Palmer, T.J. (Eds.), *Carbonate Platform Systems: Components and Interactions*. Geological Society London, Special Publication vol. 178, pp. 89–107.
- Owen, D.E., 2009. How to use stratigraphic terminology in papers, illustrations, and talks. Commissioner, North American Commission on Stratigraphic Nomenclature, 1979–2009. Voting Member, International Subcommission on Stratigraphic Classification, 1987–2009.
- Palmer, A.A., 1986. Cenozoic radiolarians as indicators of neritic versus oceanic conditions in continental-margin deposits; U.S. mid-Atlantic Coastal Plain. *Palaios* 1 (2), 122–132.
- Perri, F., Martín-Martín, M., Maaté, A., Hlila, R., Maaté, S., Criniti, S., Capobianco, W., Critelli, S., 2022. Provenance and paleogeographic implications for the Cenozoic sedimentary cover of the Ghomaride Complex (Internal Rif Belt), Morocco. *Marine and Petroleum Geology* 143, 105811.
- Pomar, L., 2001. Types of carbonate platforms: a genetic approach. *Basin Research* 13, 313–334.
- Pomar, L., Baceta, J.L., Hallock, P., Mateu-Vicens, G., Basso, D., 2017. Reef building and carbonate production modes in the west-central Tethys during the Cenozoic. *Marine and Petroleum Geology* 83, 261–304.
- Pujalte, V., Orue-Etxebarria, X., Schmitz, B., Tosquella, J., Baceta, J.L., Payros, A., Bernaola, G., Caballero, F., Apellaniz, E., 2003. Basal Ilerdian (earliest Eocene) turnover of larger foraminifera: age constraints based on calcareous plankton and  $\delta^{13}C$  isotopic profiles from new southern Pyrenean sections (Spain). In: Wing, S.L., Gingerich, P.D., Schmitz, B., Thomas, E. (Eds.), *Causes and Consequences of Globally Warm Climates in the Early Paleogene*. GSA Special Paper. Geological Society of America, Boulder, pp. 205–221.
- Raoult, J.F., 1966. La chaîne du Haouz du Col d'Azlu d'Arabia au Bab Aonzar. *Notes et Mémoires du Service Géologique du Maroc* 184, 61–146.
- Reich, S., Di Martino, E., Todd, J.A., Wesselingh, F.P., Renema, W., 2015. Indirect paleoseagrass indicators (IPSSs): a review. *Earth-Science Reviews* 143, 161–186.
- Rivero-Cuesta, L., Westerhold, T., Alegret, L., 2020. The Late Lutetian Thermal Maximum (middle Eocene): first record of deep-sea benthic foraminiferal response. *Palaeogeography, Palaeoclimatology, Palaeoecology* 545, 1–11.
- Scheibner, C., Speijer, R.P., 2008. Late Paleocene–Early Eocene Tethyan carbonate platform evolution – a response to long- and short-term paleoclimatic change. *Earth-Science Reviews* 90, 71–102.
- Serra-Kiel, J., Martín-Martín, M., El Mamoune, B., Martín-Algarra, A., Martín-Pérez, J.A., Tosquella, J., Ferrández-Cañadell, C., Serrano, F., 1998a. Biostratigraphy and lithostratigraphy of the Paleogene of the Sierra Espuña area (oriental Betic Cordillera, SE Spain). *Geologica Acta* 32 (1–3), 161–189.
- Serra-Kiel, J., Hottinger, L., Caus, E., Drobne, K., Ferrández, C., Jauhri, A.K., Less, G., Pavlovec, R., Pignatti, J., Samsó, J.M., Schaub, H., Sirel, E., Strougo, A., Tambareau, Y., Tosquella, J., Zakrevskaya, E., 1998b. Larger foraminiferal biostratigraphy of the Tethyan Paleocene and Eocene. *Bulletin de la Société Géologique de France* 169, 281–299.
- Spanicek, J., Cosovic, V., Mrinjek, E., Vlahovic, I., 2017. Early Eocene evolution of carbonate depositional environments recorded in the Cikola Canyon (North Dalmatian Foreland Basin, Croatia). *Geology of Croatia* 70, 11–25.
- Thomas, E., Shackleton, J., Knox, R.W.O.B., Corfield, R.N., Dunay, R.E., 1996. The Paleocene–Eocene benthic foraminiferal extinction and stable isotope anomalies. Correlation of the Early Paleogene in Northwest Europe. *Geological Society Special Publication* 101, pp. 401–441.
- Tomás, S., Frijia, G., Bömelburg, E., Zamagni, J., Perrin, C., Mutti, M., 2016. Evidence for seagrass meadows and their response to paleoenvironmental changes in the early Eocene (Jafnayn Formation, Wadi Bani Khalid, N Oman). *Sedimentary Geology* 341, 189–202.
- Tosquella, J., Serra-Kiel, J., 1998. Los nummulitidos (Nummulites y Assiliina) del Paleoceno Superior-Eoceno Inferior de la Cuenca Pirenaica: Sistemática. *Acta Geologica Hispánica* 31, 37–159.
- Tosquella, J., Martín-Martín, M., Guerrero, F., Francisco Serrano, F., Tramontana, M., 2022. The Eocene carbonate platform of the central-western Malaguides (Internal Betic Zone, S Spain) and its meaning for the Cenozoic paleogeography of the westernmost Tethys. *Palaeogeography, Palaeoclimatology, Palaeoecology* 589, 110840.
- Van Hinsbergen, D.J.J., Torsvik, T.H., Schmid, S.M., Matenco, L.C., Maffione, M., Vissers, R.L.M., Güreer, D., Sparkman, W., 2020. Orogenic architecture of the Mediterranean region and kinematic reconstruction of its tectonic evolution since the Triassic. *Gondwana Research* 81, 79–229.
- Westerhold, T., Röhl, U., Donner, B., Frederichs, T., Kordes, W.E.C., Bohaty, S.M., Hodell, D.A., Laskar, J., Zeebe, R.E., 2018. Late Lutetian Thermal Maximum-crossing a thermal threshold in Earth's climate system? *Geochemistry Geophysics Geosystems* 19, 73–82.
- Westphal, H., Halfar, J., Freiwald, A., 2010. Heterozoan carbonates in subtropical to tropical settings in the present and past. *International Journal of Earth Sciences (Geologische Rundschau)* 99 (Suppl. 1), S153–S169.
- Woelkerling, W.J., Irvine, L.M., Harvey, A.S., 1993. Growth-forms in non-geniculate coral-line red algae (Corallinales, Rhodophyta). *Australian Systematic Botany* 6, 277–293.
- Wright, V.P., Burgess, P.M., 2005. The carbonate factory continuum, facies mosaics and microfacies: an appraisal of some of the key concepts underpinning carbonate sedimentology. *Facies* 51, 17–23.
- Zachos, J.C., Lohmann, K.C., Walker, J.C.G., Wise, S.W., 1993. Abrupt climate change and transient climates during the Paleogene: a marine perspective. *Journal of Geology* 101, 191–213.
- Zachos, J.C., Pagani, M., Sloan, L.C., Thomas, E., Billups, K., 2001. Trends, rhythms, and aberrations in global climate 65Ma to present. *Science* 292, 686–693.
- Zachos, J., Dickens, G., Zeebe, R., 2008. An early Cenozoic perspective on greenhouse warming and carbon-cycle dynamics. *Nature* 451, 279–283.